Quaternary Science Advances 19 (2025) 100294

Contents lists available at ScienceDirect

Quaternary Science Advances

journal homepage: www.sciencedirect.com/journal/quaternary-science-advances

Biochronological and paleobiogeographic implications of the *Dama*-like deer sample from the latest Early Pleistocene of Cal Guardiola (NE Iberia)

Elpiniki-Maria Parparousi [a,*], Leonardo Sorbelli [b,c], Marco Cherin [a], Marzia Breda [d], Alessandro Blasetti [e], Marco Peter Ferretti [f], Darío Fidalgo [g], Saverio Bartolini-Lucenti [c,h], Pierre-Élie Moullé [i], Bienvenido Martínez-Navarro [j,k,l], Lorenzo Rook [h], Joan Madurell-Malapeira [h,**]

[a] Dipartimento di Fisica e Geologia, Università degli Studi di Perugia, Italy
[b] Museum für Naturkunde, Leibniz Germany Institut für Evolutions und Biodiversitätsforschung, Berlin, Germany
[c] Institut Català de Paleontologia Miquel Crusafont (ICP-CERCA), Universitat Autònoma de Barcelona, Spain
[d] Centro di Ateneo per i Musei (CAM), Museo della Natura e dell'Uomo, Università di Padova, Italy
[e] Museo delle Scienze, Università di Camerino, Italy
[f] Scuola di Scienze e Tecnologie, Sezione di Geologia, Università di Camerino, Italy
[g] Departamento de Paleobiología, Museo Nacional de Ciencias Naturales (CSIC), Madrid, Spain
[h] Dipartimento di Scienze della Terra, Paleo[Fab]Lab, Università degli Studi di Firenze, Italy
[i] Musée de Préhistoire Régionale de Menton, France
[j] Institut Català de Paleoecologia Humana i Evolució Social (IPHES-CERCA), Tarragona, Spain
[k] Àrea de Prehistòria, Universitat Rovira i Virgili (URV), Tarragona, Spain
[l] Institució Catalana de Recerca i Estudis Avançats (ICREA), Barcelona, Spain

ARTICLE INFO

Keywords:
Dama
Early-Middle Pleistocene Transition
Europe
Fallow deer
Pseudodama

ABSTRACT

Different species of *Dama*-like deer usually included in the genus *Pseudodama*, occurred in the European Plio-Pleistocene. In this paper, the medium-sized cervid sample from the Cal Guardiola Section (NE Iberian Peninsula) is described. It exhibits notable similarities with other records referred to *Pseudodama vallonnetensis* from various late Early Pleistocene European sites, thus confirming the abundance of this taxon in the faunal associations of this period. Here, we review the spatial and temporal distribution of *P. vallonnetensis* in Europe and, in a broader framework, also the succession of *Dama*-like deer species during the entire Pleistocene, analyzing variations in body size and possible relationships between these and palaeoenvironmental conditions.

1. Introduction: state of the art on Plio-Pleistocene medium-sized deer in Europe

During the Pliocene and Early Pleistocene, various medium-sized deer species with unpalmated, three- or four-pointed antlers are recorded in Europe (Azzaroli, 1947, 1992, 2001; Heintz, 1970; Pfeiffer-Deml, 2016; Croitor, 2018; Breda et al., 2020; Cherin et al., 2022). Although most of these species were initially referred to the genus *Cervus* in its broad sense (e.g., *C. pardinensis*, *C. philisi*, *C. perolensis*), they are currently considered to be related to the extant fallow deer (genus *Dama*) as they exhibit several morphological similarities in their antlers, skull, teeth and postcranial elements (Breda et al., 2020; Cherin et al., 2022), and are therefore commonly collectively referred to as "*Dama*-like deer", term first introduced by Di Stefano and Petronio (1998). The taxonomy of *Dama*-like deer is still a matter of dispute (Pacheco et al., 2011; Made, 2013; Made et al., 2014; Cherin et al., 2022), as the available samples have been attributed to a plethora of different genera, such as *Axis*, *Dama*, *Euraxis*, *Metacervocerus*, *Pseudodama*, *Preelaphus*, or *Rusa*, in mere alphabetical order (e.g., de Lumley et al., 1988; Azzaroli, 1992; Di Stefano and Petronio, 1998, 2002; Petronio et al., 2013; Pfeiffer-Deml, 2016; Croitor, 2018; Cherin et al., 2019, 2022; Breda et al., 2020).

Heintz (1970) attributed some of them to the genus *Cervus* s.l. and suggested a single lineage comprising the species *C.* s.l. *pardinensis* (=*P.*

* Corresponding author.
** Corresponding author.
E-mail addresses: elpinikimaria.parparousi@dottorandi.unipg.it (E.-M. Parparousi), joan.madurellmalapeira@unifi.it (J. Madurell-Malapeira).

https://doi.org/10.1016/j.qsa.2025.100294
Received 24 January 2025; Received in revised form 29 June 2025; Accepted 11 August 2025
Available online 18 August 2025

pardinensis) – *C.* s.l. *philisi* (=*P. rhenana* = *P. philisi*) – *C.* s.l. *perolensis* (=*P. perolensis*).

Azzaroli (1992) included all Villafranchian (ca. 3.3–1.2 Ma) *Dama*-like deer within the genus *Pseudodama*. Rather unexpectedly, Azzaroli (1992) did not even mention in this review the medium-sized cervid sample from the French site of Le Vallonnet first described as "*Cervus*" *nestii vallonnetensis* by de Lumley et al. (1988). The same sample was later referred to *Dama vallonnetensis* by Croitor (2001) and to *P. nestii vallonnetensis* by Moullé et al. (2006). Azzaroli (2001) indicated that the specimens described by himself in an earlier work (Azzaroli, 1947) as *Dama nestii eurygonos*, i.e. a subspecies within *Dama nestii,* rather represent the adult morphological stage of *Dama nestii* (=*Pseudodama nestii*), whose type material would correspond to an earlier ontogenetic stage. For this reason, the taxon *Dama nestii eurygonos* was omitted from the genus *Pseudodama* in Azzaroli (1992).

According to the most recent works (Cherin et al., 2022), the European species of this genus in chronological order are therefore *Pseudodama pardinensis*, *Pseudodama lyra*, *Pseudodama rhenana*, *Pseudodama nestii* (i.e., the genotype species), *Pseudodama farnetensis*, *Pseudodama perolensis*, and *Pseudodama vallonnetensis*. Azzaroli (1992) suggested the existence of two anagenetic lineages, one, limited to Italy, composed by *P. lyra* – *P. nestii* – *P. farnetensis*, and one, limited to France, composed by *P. pardinensis* – *P. philisi* (=*P. rhenana*) – *P. perolensis*. In the same paper, Azzaroli states that an anagenetic evolutionary trajectory from *Pseudodama* to *Dama* seems unlikely given the absence of evidence of intermediate morphological traits such as palmation and the divergent antler morphology observed in *Pseudodama farnetensis*. Several authors recognized an evolutionary trend along both lineages in the antler morphology, which shows a progressive (1) approach of the basal tine towards the burr; (2) opening of the angle between the basal tine and the beam; (3) change in the orientation of the terminal fork with respect to the sagittal plane of the skull (e.g., Azzaroli, 1992; Made, 1999; Petronio et al., 2013).

Vos et al. (1995) stated that the species *Pseudodama lyra* Azzaroli (1992) is a junior synonym of *Cervus rhenanus* Dubois, 1904, whereas Croitor (2006) considered *P. lyra* as a junior synonym of *P. nestii* and moved it in the genus *Cervus*. However, in later works, Croitor (2012, 2018) resurrected *P. lyra* as a valid species and moved it into the genus *Preelaphus*.

Di Stefano and Petronio (1998) suggested that the Italian lineage of Azzaroli's genus *Pseudodama* shares a phylogenetic link with the Asian species *Axis axis*, thus referred the Italian *Dama*-like deer to the genus *Euraxis*, and later to the genus *Axis* (Di Stefano and Petronio, 2002). The same authors suggest that the species of the French lineage of *Pseudodama*, would be related to the modern genus *Rusa* (Di Stefano and Petronio, 1998) or even be part of it (Di Stefano and Petronio, 2002). In contrast to this, Croitor (2006) suggested that *Metacervoceros rhenanus* (and thus the best represented species of the French lineage) is a primitive deer similar to modern *Axis*.

Pfeiffer (2005) included some species of the group into the genus *Dama* (*D. lyra*, *D. pardinensis*, *D. rhenana* and *D. nestii*) and suggested they are the direct ancestors of *D. dama clactoniana*, *D. dama geiselana* and the extant fallow deer. However, in her publication, the Pirro Nord sample of *Dama*-like deer is considered as *Axis* sp. and forms a clade with *Axis axis* that is sister taxon to the *Dama* clade (majority-rule consensus tree in Pfeiffer, 2005: fig. 4).

Croitor (2006) suggested that several *Dama*-like deer species do not constitute a monophyletic group and instead belong to several different genera (*Cervus*, *Dama*, *Metacervoceros*). Although acknowledging the unclarity of the phylogenetic relationships among the Plio-Pleistocene and modern fallow deer, the latter author suggested that *Dama eurygonos* and *Dama vallonnetensis* belong to the same lineage, with modern fallow deer representing a separate lineage. In addition, he suggested that *Pseudodama* is a junior synonym of the genus *Cervus*, and that the species *Metacervocerus pardinensis* and *Metacervocerus rhenanus* differ from modern *Dama* in having three pointed antlers, longer and caudally inclined pedicles as well as a more primitive dental morphology, among other characters.

Breda and Lister (2013), Breda (2015) and Cherin et al. (2023) follow Azzaroli (1992) by including all the forms of the *Dama*-like group under the genus *Pseudodama*, and hypothesize that this group may form a paraphyletic stem group in the fallow deer clade.

Similarly to Pfeiffer (2005), Made (2015) and Made et al. (2014, 2017) include most *Dama*-like deer in the genus *Dama*. Made (2001) suggested that the species *P. nestii* and *P. vallonnetensis* belong to a phyletic line leading to the extant fallow deer, whereas Made et al. (2023) suggested the lineage *D. farnetensis–D. vallonnetensis–D. roberti–D. celiae*.

Finally, the phylogenetic study of Cervidae by Heckeberg (2020) did not include all known *Dama*-like deer species and provided unresolved data for those considered (i.e., different positions of these species with respect to extant ones in phylogenetic trees obtained with different methods).

In order to further address the complex and heterogeneous taxonomic and systematic history of the group we have compiled a comprehensive table (Supplementary Table 1), that presents the interpretations of different authors for the whole European *Dama*-like deer record.

Here, following the taxonomy of Azzaroli (1992), we include all Villafranchian and Epivillafranchian (ca. 3.3–0.8 Ma) *Dama*-like deer within the genus *Pseudodama*, in line with many other authors (e.g., Abbazzi et al., 1995; Moullé et al., 2006; Breda and Lister, 2013; Bona and Sala, 2016; Breda et al., 2020; Cherin et al., 2022; Mecozzi et al., 2023; Konidaris and Kostopoulos, 2024). Although we acknowledge the lack of a conclusive phylogenetic framework, our taxonomic choice is guided by the principle of maximum parsimony and the awareness that all *Dama*-like deer forms share with modern *Dama* several key morphological characters in antlers, teeth and postcranial elements. So, while keeping the Villafranchian and Epivillafranchian *Dama*-like deer in *Pseudodama*, distinct from modern *Dama* because of the complete lack of palmation in their three- or four-pointed antlers, we are aware that the lack of palmation is most probably a plesiomorphic character (Pfeiffer, 2005; Breda and Lister, 2013) and so *Pseudodama* is probably a paraphyletic stem group.

In this current work we mainly focus on the most derived form of the genus *Pseudodama*, namely *Pseudodama vallonnetensis*. A rich sample referred to this species was described from Untermassfeld in Germany as *Cervus* s.l. *nestii vallonnetensis* (Kahlke, 1997, 2001) then moved to '*Pseudodama' vallonnetensis* by Breda et al. (2020). The sample from Pirro Nord (Italy), formerly attributed to *Axis eurygonos* (Petronio et al., 2013) and to *Dama vallonnetensis* (Croitor, 2014, 2018), also belongs to the same species. Other more fragmentary samples of *P. vallonnetensis* were reported from Collecurti [Italy; *Dama nestii* in Ficcarelli and Mazza (1990); *"Cervus" nestii vallonnetensis* in Ficcarelli and Silvestrini (1991); *Pseudodama* ex gr. *nestii* in Mazza and Ventra (2011)], Arda River [Italy; *P. farnetensis* in Bona and Sala (2016), erroneously considered as a junior subjective synonym to *P. vallonnetensis*], and other sites (see Cherin et al., 2022 for a review).

Here, we discuss the taxonomy and biochronological and paleoenvironmental significance of the *Dama*-like deer record from Cal Guardiola local section (NE Iberia; Madurell-Malapeira et al., 2010), also considering and reviewing data on unpublished and published samples of almost coeval age from Europe. The sites taken into consideration are depicted in Fig. 1.

2. Geological, chronological, and paleoenvironmental background

2.1. Geological and chronological background

The Vallparadís Section encompasses the paleontological sites of Cal Guardiola (CGR) and Vallparadís Estació (EVT), situated in the Vallès-

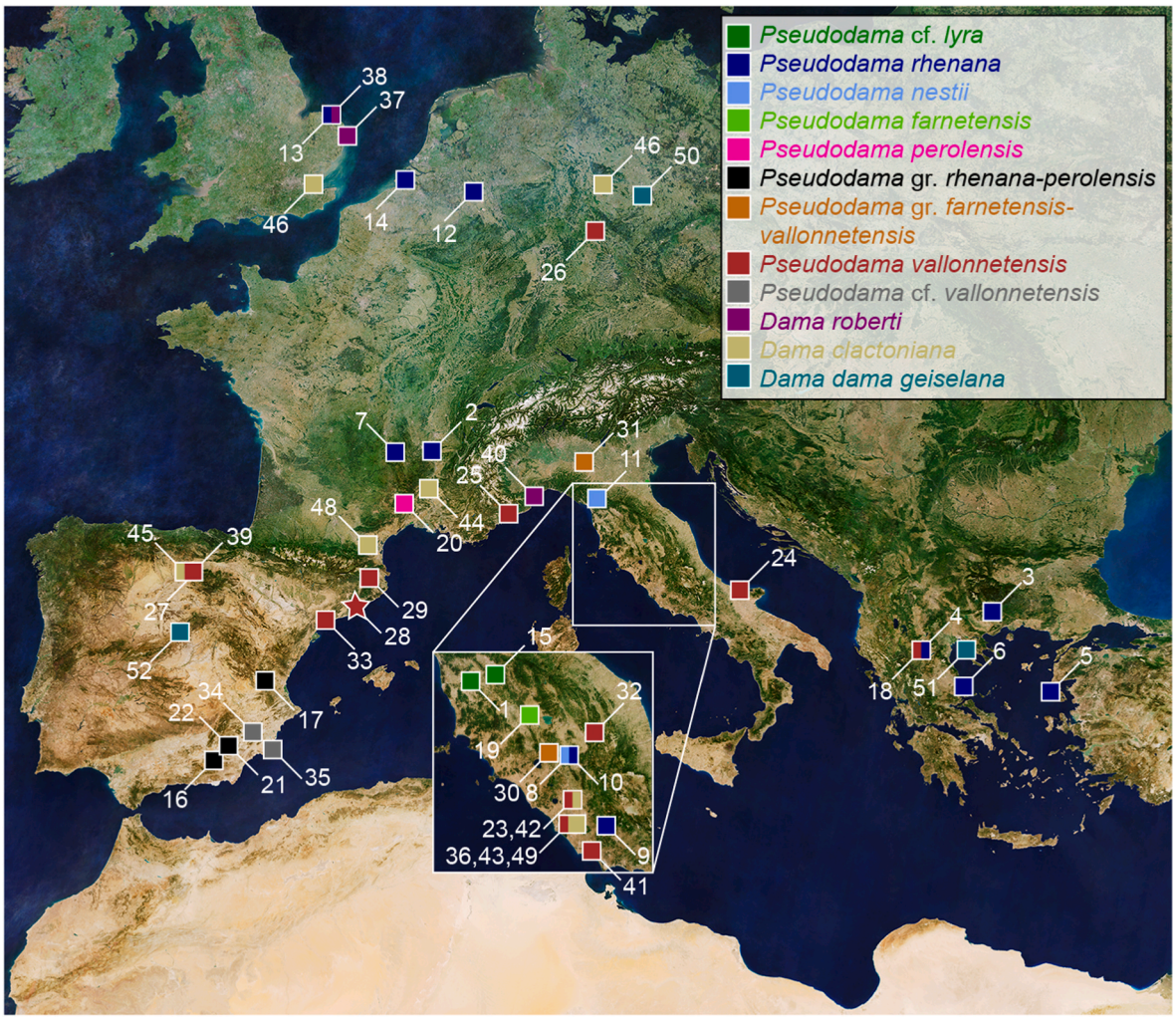

Fig. 1. Map of European sites taken into consideration (Cal Guardiola is indicated by a star): 1, Montopoli; 2, Saint Vallier; 3, Volax; 4, Dafnero; 5, Vatera; 6, Sesklo; 7, Senèze; 8, Pantalla; 9, Coste San Giacomo; 10, Cava Toppetti; 11, Olivola; 12, Tegelen; 13, East Runton; 14, Oosterschelde; 15, Valdarno Sites; 16, Venta Micena; 17, Alto de las Picarazas; 18, Libakos; 19, Val di Chiana sites; 20, Peyrolles; 21, Barranco León; 22, Fuente Nueva 3; 23, Capena; 24, Pirro Nord; 25, Le Vallonnet; 26, Untermassfeld; 27, Sima del Elefante TE9-7 and Trinchera Dolina TD6-4 (Atapuerca Complex); 28, Cal Guardiola; 29, Can Jan (Incarcal Complex); 30, Monte Peglia; 31, Frantoio; 32, Collecurti; 33, Barranc de la Boella; 34, Cueva Negra del Estrecho del Río Quipar; 35, Cueva Victoria; 36, Cava Redicicoli; 37, Pakefield; 38, West Runton; 39, Trinchera Dolina TD8 (Atapuerca Complex); 40, Valdemino Cave; 41, Nettuno; 42, Riano; 43, Tor di Quinto; 44, Caune del'Arago; 45, Trinchera Dolina TD10 (Atapuerca Complex); 46, Bilzingsleben; 47, Swanscombe; 48, Orgnac 3; 49, Vitinia; 50, Neumark Nord; 51, Petralona; 52, Pinilla del Valle.

Penedès Basin in northeastern Iberia (Madurell-Malapeira et al., 2010, 2017, 2024). Over the course of emergency excavations conducted from 1997 to 2008 following different phases of large construction works, these sites yielded more than 30,000 vertebrate remains dating from the late Early to Middle Pleistocene. Both locations exhibit a distinctive depositional setting influenced by the dynamics of an alluvial fan system and the geometry of the Miocene paleorelief.

Biochronological, magnetostratigraphic, and U-series-ESR data collectively indicate that the Vallparadís Section spans from before the Jaramillo paleomagnetic subchron (ca. 1.2–1.1 Ma; MIS 35) to the early Middle Pleistocene (ca. 0.6 Ma; Madurell-Malapeira et al., 2010, 2012, 2014, 2017; Minwer-Barakat et al., 2011).

The specimens under investigation in this study were extracted from the pre-Jaramillo layers (ca. 1.2–1.1 Ma; MIS 35) and the post-Jaramillo, Matuyama layers (ca. 0.86 Ma; MIS 21) of the Cal Guardiola Section (Madurell-Malapeira et al., 2010, 2014, 2017, 2024; Sorbelli et al., 2021).

2.2. Paleoclimatic and paleoenvironmental background

Throughout the Pliocene and Pleistocene, long-term trends of climatic cooling and increasing glacial cycle amplitude are suggestive of significant changes in the dynamics of the Earth climate system (Lisiecki and Raymo, 2007). Additionally, a trend towards aridification and increasing seasonality in Europe throughout the Pleistocene is generally accepted (Head and Gibbard, 2015), forcing a progressive transition from tropical-subtropical ecosystems to present-day ones (Bertini et al., 2010; Magri et al., 2017). Of course, such transition did not occur abruptly but rather progressively and non-linearly, through a series of fluctuating environmental changes driven by glacial-interglacial cycles. Since approximately 1.4 Ma there has been a progressive increase in climate oscillation amplitude, a shift from a 41-ka to quasi-100-ka orbital rhythm, a sustained increase in long-term average ice volume, and the establishment of a pronounced asymmetry in glacial ice volume cycles, marking the '*Early-Middle Pleistocene Transition*' (EMPT) as defined by Head and Gibbard (2015). In response to the aforementioned changes, the European large mammal assemblages have progressively been enriched – albeit with fluctuations in diversity – with species more adapted to open environments coinciding with the first hominin dispersal in the continent (Leroy et al., 2011; Sorbelli et al., 2023). This faunal reorganization was recognized by European paleontologists as marking the transition between the Villafranchian and Epivillafranchian

biochrons in the large mammal-based biochronological scheme of the continent (Kahlke et al., 2011; Bellucci et al., 2015).

All the above transitions are well visible in the Vallparadís Section. Pollen and wood analysis from CGRD2 (ca. 1.2–1.1 Ma; MIS 35) indicates a warm-temperate and humid paleoenvironment, suggestive of a river or river-marsh ecosystem hosting diverse plant groups ranging from aquatic macrophytes to deciduous trees and grasses. The prevalence of hippo remains in this layer aligns with the inferred fluvial/lacustrine main depositional environment, while the high diversity of large-sized ungulates, such as deer, horses, and bison, suggests a varied landscape encompassing woodlands and more open, dry areas (Mijarra et al., 2007). Meso- and microwear analyses conducted on a substantial sample of ungulate teeth from the section (Strani et al., 2019) indicate a noteworthy shift in paleoenvironments since 0.9 Ma (MIS 22). Initially dominated by open, dry grasslands with discernible seasonality (layer EVT12; ca. 1.0 Ma; MIS 30), the environment transitioned to more humid woodlands, possibly with an even more pronounced seasonality (layers EVT7 and CGRD7; ca. 0.86–0.78 Ma; MIS 21). These findings align with data from other contemporaneous Southern European sites (Strani et al., 2019). Preliminary investigations into the stable isotopic signal from layers EVT12 and EVT7 also suggest a period of increased aridity during the Jaramillo subchron and more wooded environments during MIS 21 (Vizcaíno-Varo, 2023). According to Strani et al. (2019) *Dama*-like deer through the Section display predominantly grazing diet during MIS 30 changing to mixed-feeder at MIS 21. These last results were reinforced with the preliminary data on stable isotopes which indicates a diet with outstanding plasticity for the *Dama*-like deer of MIS 30 and MIS 21 (Vizcaíno-Varo, 2023).

3. Materials and methods

The *Dama*-like deer sample from Cal Guardiola studied herein is housed in the Institut Català de Paleontologia Miquel Crusafont (ICP), Barcelona, Spain. The list of specimens is reported in Supplementary Table 2. Standard measurements were recorded to the nearest 0.1 mm with a digital caliper and are provided in Supplementary Tables 3–19. Measurements were taken following Driesch (1976), Breda et al. (2020), and Sorbelli et al. (2021). Comparative morphological and biometric data were taken from the following papers: Petronio (1979), Catalano (1983), Menéndez (1987), de Lumley et al. (1988), Azzaroli (1992), Vos et al. (1995), Kahlke (1997), Mancini et al. (2008), Abbazzi (2010), Lister et al. (2010), Breda and Lister (2013), Petronio et al. (2013), Made et al. (2014; 2017), Breda (2015), Made (2015), Croitor (2018), Breda et al. (2020), Cherin et al. (2022), Mecozzi et al. (2023), Strani et al. (2024). In addition, original data were collected from the following samples: *P. rhenana* from Senèze (Université Claude Bernard Lyon-1); *P. nestii* from Olivola and Upper Valdarno (Museo di Storia Naturale, Sezione di Geologia e Paleontologia, Università di Firenze); *P. farnetensis* from Val di Chiana (Museo di Storia Naturale, Sezione di Geologia e Paleontologia, Università di Firenze); *P.* gr. *farnetensis-vallonnetensis* from Cava Redicicoli (Museo di Scienze della Terra, Sapienza Università di Roma); *P. perolensis* from Peyrolles (The Natural History Museum, London); *P.* gr. *rhenana-perolensis* from Venta Micena, Barranco León and Fuente Nueva 3 (Museo Arqueológico de Granada); *P. vallonnetensis* from Capena (Museo di Scienze della Terra, Sapienza Università di Roma); *P. vallonnetensis* from Pirro Nord (Dipartimento di Scienze della Terra, Università di Firenze); *P. vallonnetensis* from Le Vallonnet (Musée de Préhistoire Régionale de Menton); *P. vallonnetensis* from Untermassfeld (Senckenberg Forschungsstation für Quartärpaläontologie Weimar); *P. vallonnetensis* from Incarcal Complex (Can Jan) (Museu Arqueològic Comarcal de Banyoles); *P. vallonnetensis* from Collecurti (Museo delle Scienze, Università di Camerino); *P. vallonnetensis* from Barranc de la Boella (Institut Català de Paleoecologia Humana i Evolució Social); extant *Dama dama* from Spain (Museu Ciències Naturals de Barcelona). Data sources are summarized in Supplementary Table 20. The anatomical terminology follows Heintz (1970) (mainly for dental characters) and Lister (1996) (for dental and postcranial characters). The investigation of *Cervus*-like and *Dama*-like characters follows Lister (1996), in line with previous works on *Dama* and *Dama*-like deer samples (e.g., Breda and Lister, 2013; Made et al., 2014; Stefaniak, 2015; Breda et al., 2015, 2020; Cherin et al., 2022; Rosas et al., 2022; Mecozzi et al., 2023; Valli, 2025), as well as personal observations on cranial morphology. Juvenile specimens were not included in the metrical analyses. The statistical analysis was conducted with PAST v. 4.13 (Hammer et al., 2001). Body mass estimations were obtained following Janis (1990) and particularly using the following regression equation ("Selenodont browsers" in table 16.9): $x = 10^{[(2.88 \times \mathrm{Log}_{10} y)+1.81]}$, where x is the body mass in kg and y is the m3 width in cm. We chose m3 width as a proxy of body dimensions following Made et al. (2014) and Made et al. (2017). We hereby refer to all *Dama*-like deer specimens exhibiting derived characters, which cannot be certainly attributed to either *P. farnetensis* or *P. vallonnetensis* due to the scanty and fragmentary nature of the material, as *P.* gr. *farnetensis-vallonnetensis.* Similarly, some Iberian samples of uncertain taxonomy are hereby referred to as *P.* gr. *rhenana-perolensis*.

4. Results

4.1. Referred specimens

See Supplementary Table 2.

4.2. Measurements

See Supplementary Tables 3–19

4.3. Description

Cranium—The cranium IPS13558, belonging to an incomplete skeleton (Fig. 2) is quite complete but severely deformed, due to lateral compression, lacking several parts (Fig. 3 a1-a2). The left side is better preserved than the right one, preserving most of the neurocranium, the orbit and zygomatic arch, and part of the splanchnocranium including the posterior portion of the nasal and most of the maxilla with P2-M3 (complete P2-P4, paracone of M1, displaced metacone of M2, and complete M3). Dorsal to the posterodorsal corner of the orbit, damage of the cortical bone exposes a thick portion of the frontal that can be interpreted as the postorbital bar. This, associated with the overall thickening of the frontals visible in the area between the orbits, suggests the former presence of pedicles, hence the identification of the individual as a male. The braincase is relatively short, with a rounded dorsal outline. Above the nearly circular orbit, the frontal slopes forming a smooth forehead. The temporal fossa is elongated, wide, and with a convex surface. When the cranium is viewed laterally with the cheek tooth row parallel to the horizontal plane, the akrokranion extends posteriorly about at the same level as the posterior margin of the occipital condyles. The left zygomatic arch is short, thin, and almost horizontal, parallel to the cheek tooth row. The external auditory meatus is directed dorsolaterally. The (damaged) postorbital bar forms an angle of about 45° with the sagittal axis. Anteriorly to the orbit, both the preorbital fossa and ethmoidal vacuity are poorly preserved. The posterior part of the nasal seems stout, but its original position is altered by deformation. The maxilla is stout and broken anteriorly at the level of a wide infraorbital foramen, placed above the mesial margin of P2.

Antlers—The Cal Guardiola collection includes 88 antler specimens, but none are complete (Fig. 3b–l). Of the available specimens, 82 preserve basal portions broken before the terminal fork and six are represented by fragmented tines of the terminal fork. The maximum length of preserved beam is estimated at about 273 mm (specimen IPS13910; Fig. 3h), whereas the maximum length of preserved tine of the terminal fork is estimated at about 254 mm (specimen IPS16845; Fig. 3f). All non-juvenile antlers from Cal Guardiola show strong furrows and ridges

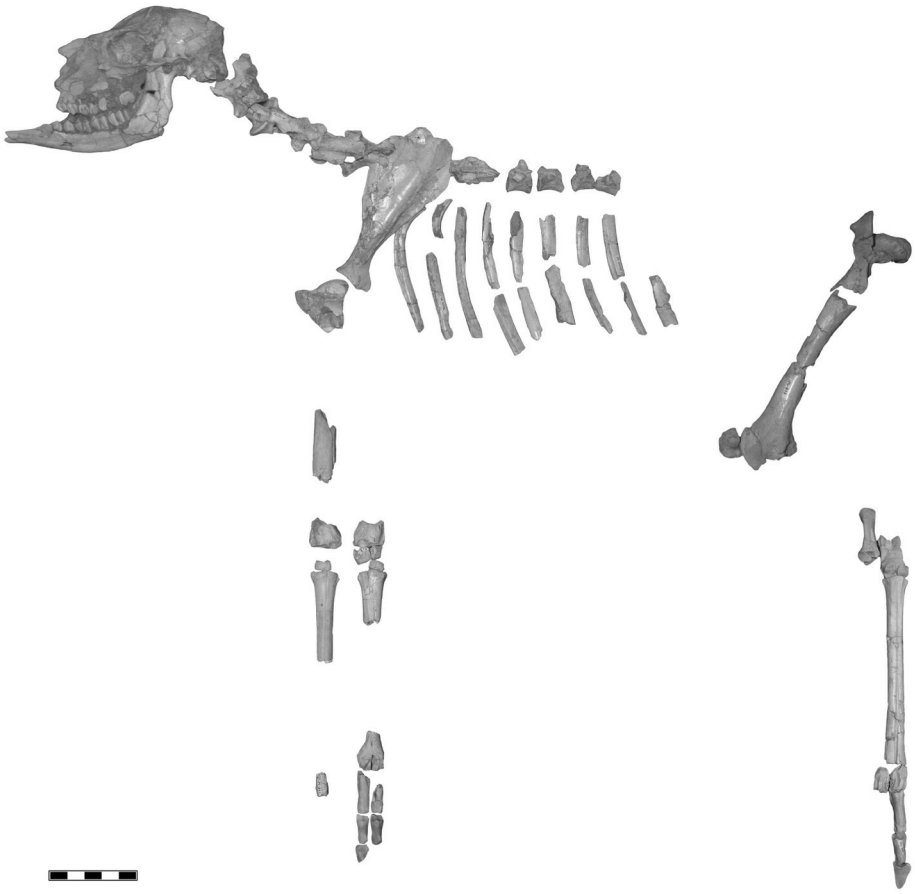

Fig. 2. Partial skeleton of *Pseudodama vallonnetensis* from Cal Guardiola layer CGRD5. Scale bar: 10 cm.

along the beam and the basal tine (Fig. 3g). The pedicle is relatively low in the adult specimens (posterior height of pedicle: 13.22–23.26 mm); however, it is longer in juvenile specimens (20.29–26.9 mm). The burr is strong, evenly developed and it has an oval/subcircular outline. The proximal part of the beam is directed dorsolaterally and posteriorly (in early ontogenetic stages, the beam is more vertical, overall; e.g., Fig. 3g). The basal tine is placed right above the burr. It emerges straight and then exhibits an upward curvature that can vary from an abrupt bend (e.g., IPS770; Fig. 3c) to a smoother curve (e.g., IPS13447), often inclining slightly towards the midline. This curvature typically begins beyond the midpoint of the tine's length (the position of the curvature is variable, as it can start at the exact midpoint of the tine's length or towards its end, e.g., IPS770; Fig. 3c). The angle between the basal tine and the beam is obtuse in most of the specimens, as it varies from 80° to 150° with a mean value of 119° (n = 18) (Supplementary Fig. 1). Overall, the angle increases with aging, together with the tendency towards horizontalization of the beam (see above). No evidence of intermediate tines has been detected in any antlers from CGR, even in the largest preserved antler portions (e.g., specimen IPS13910; Fig. 3h). The tines of the terminal fork have a relatively oval (slightly mediolaterally compressed) outline. No specimens show any palmation.

Mandible— The corpus is slender and elongated and the diastema between c1 and p2 is long. The coronoid process is mediolaterally flattened, and it projects dorsocaudally. The mandibular (sigmoid) notch is a deep and narrow concave groove, delimited anteriorly by the coronoid process and posteriorly by the condyle. The ascending ramus is quite high relative to the hemimandible as a whole and forms an obtuse angle (about 110°) with the corpus. The dorsal and ventral margins of the corpus are curved and convergent towards the anterior part. However, we note that specimens IPS13558 (Fig. 3a) and IPS18501 (Fig. 4e) present a dorsoventrally thinner mandibular corpus than IPS14919 (Fig. 4c).

Upper teeth—In occlusal view, P2 and P3 are morphologically similar to each-other and both molarized, since we note a lingual notch separating each tooth into a mesial and distal lobe (protocone and hypocone, respectively). This notch is deeper in the P2 (e.g., IPS20165). The buccal styles, especially the metastyle, are well developed; the metastyle projects distobuccally. The left P4 of cranium IPS13558 is the only preserved P4 in CGR (Fig. 3a2). The specimen can only be observed in buccal view; thus, no particular morphological inferences can be drawn. The upper molars are mesiodistally compressed, attaining an almost squared outline in occlusal view (IPS14930, Fig. 4f). They have weak cingula on the lingual side (the cingulum tends to be stronger in M1 and shorter in M3). In all upper molars, the entostyle is well developed.

Lower teeth—No p2 are preserved in the CGR collection. The p3 of IPS18501 (Fig. 4e) has less pronounced parastylid and paraconid and a narrower valley than that of IPS14919 (Fig. 4c). The paraconid and parastylid of p3 in the former specimen are not well divided also in lingual view, whereas, in the latter specimen, they are better separated along the upper part of the crown. The parastylid of this latter specimen is moderately developed. The second valley is often wide (e.g., IPS18501), due to the distal shifting of the metaconid (Fig. 4e). The entoconid and entostylid are divided only on the upper part of the crown by the fourth valley. The p4 is molarized. The paraconid and metaconid of p4 are almost fused, thus closing the second valley. The molarization degree of p4 is variable, since the direction of the entoconid can be varied from oblique (e.g., IPS18501, Fig. 4e) to more aligned to the mesiodistal axis (e.g., IPS864, Fig. 4a), closing the fourth valley. The lower molars show strongly developed ectostylids in buccal view, between the mesial and the distal lobe; m3 also presents a posterior ectostylid, right between the distal lobe and the hypoconulid. In lower molars with low degree of wear (e.g., IPS61338, Fig. 4d), an opening is

Fig. 3. Cranium and antlers of *Pseudodama vallonnetensis* from Cal Guardiola. a, Cranium IPS13558 in right lateral (a1) and left lateral (a2) views; b, left antler IPS23400 in medial view; c, right(?) antler IPS770 in medial view; d, left antler IPS14963 in medial view; e, right antler IPS23401 in medial view; f, tine of terminal fork IPS16845 in medial/lateral view; g, right antler IPS14816 in medial view; h, right antler IPS13910 in medial view; i, basal tine IPS14992 in medial/lateral view; j, left antler IPS61876 in medial view; k, right antler IPS16846 in lateral view; l, right antler IPS14928 in medial view. Scale bar: 5 cm.

visible between the ectostylid and hypoconid distal wing.

Scapula—The glenoid cavity is subcircular, with the major axis anteroposteriorly oriented (Fig. 5a1, b, c). The tuber scapulae projects anteriorly of the glenoid cavity; the groove formed on the medial side of the tuber scapulae opens into the glenoid cavity and forms a dip in the margin of the glenoid cavity. This dip does not disrupt the articular surface of the glenoid cavity. The spine, when viewed from the distal end, projects laterally.

Humerus—The proximal epiphysis consists of one lateral and one medial tuberosity, separated by the intertuberal groove. The distal epiphysis consists of a large trochlea, divided by a sagittal groove located approximately in the middle between the medial and lateral condyles (Fig. 5d). The medial margin of the trochlea is proximodistally higher than the lateral one and thus, the trochlea in anterior view tapers laterally. In IPS13372, a large and bulging trochlear crest is well preserved on the lateral margin of the trochlea. In anterior view, right

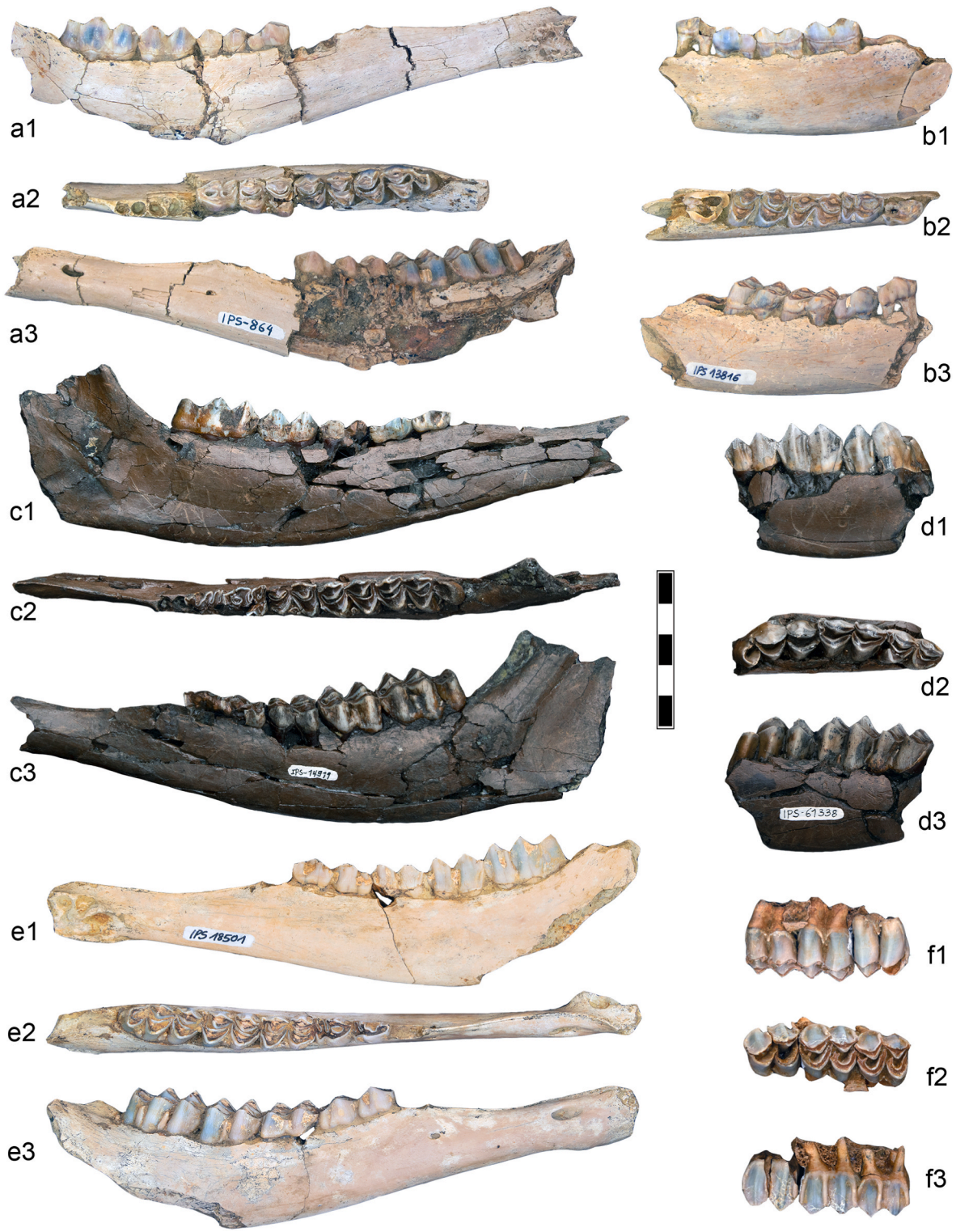

Fig. 4. Dentognathic remains of *Pseudodama vallonnetensis* from Cal Guardiola. a, Left hemimandible IPS864 with p4-m3 in (a1) lingual, (a2) occlusal, and (a3) buccal views; b, right hemimandible IPS13816 with p3-m2 in (b1) lingual, (b2) occlusal, and (b3) buccal views; c, left hemimandible IPS14919 with p3-m3 in (c1) lingual, (c2) occlusal, and (c3) buccal views; d, right hemimandible IPS61338 with m1-m3 in (d1) lingual, (d2) occlusal, and (d3) buccal views; e, right hemimandible IPS18501 with p3-m3 in (e1) lingual, (e2) occlusal and (e3) buccal views; f, right maxilla IPS14930 with M1-M3 in (f1) lingual, (f2) occlusal, and (f3) buccal views. Scale bar: 5 cm.

proximally to the distal trochlea, the coronoid and the radial fossae are visible, that is, two mediolaterally elongated depressions, which are barely divided and almost of equal size. The olecranon fossa, located in the posterior side, right proximally to the distal epiphysis, is formed by the conjunction of the lateral and medial margins, that gradually and gently become convergent towards the proximal part, until they create a smooth proximal edge and an overall ovoidal shape. The olecranon fossa is wide and short. The condyloid crest is located on the lateral surface of the shaft, right proximally of the lateral epicondyle.

Radius-ulna—The posterior outline of the proximal articulation of the

Fig. 5. Forelimb remains of *Pseudodama vallonnetensis* from Cal Guardiola. a, Left scapula IPS23423 in (a1) distal, (a2) medial, and (a3) lateral views; b, left scapula IPS14974 in distal view; c, right scapula IPS13516 in distal view; d, right humerus IPS13372 in (d1) distal, (d2) anterior, and (d3) posterior views; e, left radius and ulna IPS14942 in (e1) posterior, (e2) proximal, and (e3) distal views; f, left radius IPS14991 in (f1) anterior and (f2) posterior views; g, right metacarpal IPS16793 in (g1) proximal, (g2) distal, (g3) anterior, and (g4) posterior views. Scale bar: 5 cm.

radius is slightly undulated, forming an acute angle to accommodate the lateral articular facet of the ulna (Fig. 5f). The proximal epiphysis composes of two main facets: the medial one, for the medial epicondyle of the distal epiphysis of the humerus, with an outline that varies from trapezoid (IPS14942) to subrectangular (IPS13525), and the lateral one, for the lateral epicondyle of the distal epiphysis of the humerus, with a subtriangular outline. On the anterior border of the proximal epiphysis, a wide and broad depression between the medial and lateral facets is formed. A tuberosity is present on the lateral side of the proximal epiphysis, laterally to the lateral glenoid cavity/lateral facet; the anteroposterior diameter of this tuberosity is considerably greater than its proximodistal one. The distal epiphysis slopes posteriorly, and it composes of two main elongated facets for the carpals, which have an anterolateral to posteromedial direction (Fig. 5e). On the medial surface of the distal end, we note a weakly developed tuberosity that serves for the attachment of the medial carpal ligament. On the anterior surface of the distal epiphysis there is a grooved area for the extensor tendon, formed between a lateral and a medial ridge, running parallel to the diaphysis. This groove seems not to be delimited only in the area of the distal epiphysis, but to proceed for few centimeters proximally, in the distal diaphysis.

Metacarpals—All the studied metacarpals are slender. The proximal and distal epiphyses have more or less the same mediolateral width (Fig. 5g). Two of the CGR metacarpals (IPS14632, IPS13544) can be referred to juvenile individuals due to their unfused distal epiphyses. The proximal articular surface of the metacarpal displays a D-shaped outline in proximal view. The lateral articular facet is triangular and located on a lower plane than the medial articular facet. The two facets are separated by a crest, which, depending on the specimen, has a different degree of inclination, with an anterolateral to posteromedial direction. The medial facet is larger and subsquared, with the medial outline varying from subcircular to squared. The proximal synovial fossa has a variable outline. The proximal nutrient foramen is located at the posterior margin of the crest that separates the two facets of the proximal epiphysis, and is oval-shaped. In the juvenile specimen IPS13544, the proximal nutrient foramen is also oval-shaped, but it is connected with a furrow in its posterior part, that leads to the posterior edge of the proximal epiphysis. The proximal nutrient foramen is located more or less in the middle of the shaft, with a tendency towards the lateral part. In the posterior surface of the diaphysis, right distally of the proximal epiphysis, we note a posterior foramen, which is not connected with the foramen of the proximal epiphysis. The posterior portion of the diaphysis is characterized by a smooth and deep concave surface. In anterior view, the diaphysis appears slender and smooth. The vascular groove, which is always shallow and narrow, has its deepest part right proximally to the distal epiphysis and it runs all along the diaphysis. The distal anterior foramen is drop-shaped and is located within the vascular groove, just proximally of its end, right before the distal epiphysis. In the distal epiphysis, the trochlear crests are parallel to the main axis of the bone. The edge of the lateral epicondyle is not parallel to the sagittal axis, as it slants laterally.

Femur—The bone has a slender appearance. The femoral head has a rather smooth and convex surface, supported by a relatively high femoral neck (Fig. 6a). The greater trochanter is a rather flat, roughened projection. The lesser trochanter is a smooth, rounded eminence. The posterior side of the distal end consists of a lateral and a medial condyle, with the former being larger than the latter. The two condyles are delimited by an intercondylar fossa, whose borders are rather oblique to the sagittal plane. In posterior view, the outline of the medial condyle appears to be ovoidal, whereas that of the lateral condyle is more rounded.

Tibia—The shaft has a slender appearance. The only distal portion belongs to specimen IPS23412, which only retains the posterolateral surfaces, including the two lateral facets for the malleolar articulation, thus no particular morphological inferences can be drawn. In the anterior view of the proximal end, the tibial crest tuberosity has an oval

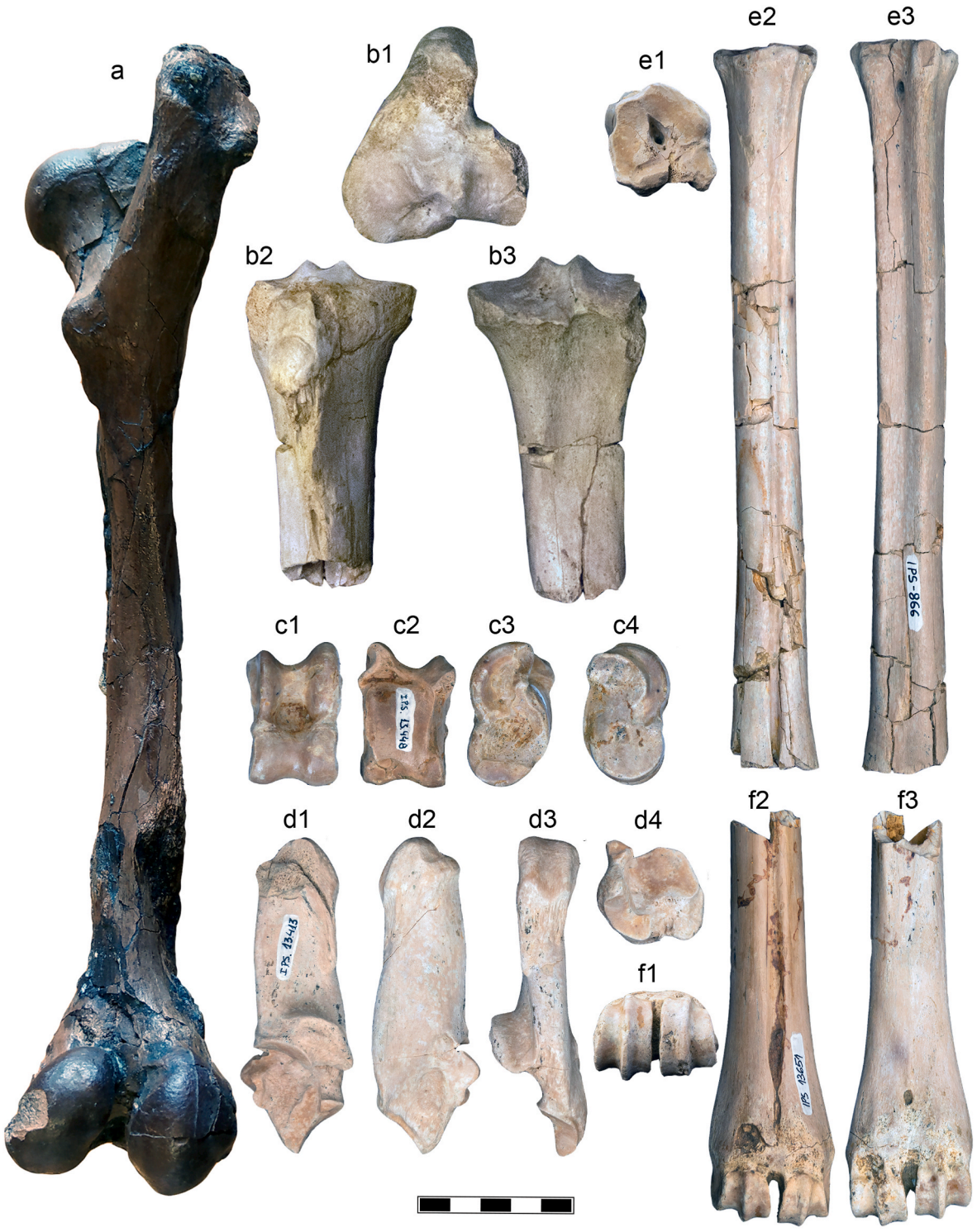

Fig. 6. Hindlimb remains of *Pseudodama vallonnetensis* from Cal Guardiola. a, Femur P.70-Nv.M-1215 in posterior view; b, right tibia IPS39125 in (b1) proximal, (b2) anterior, and (b3) posterior views; c, left astragalus IPS13448 in (c1) anterior, (c2) posterior, (c3) lateral, and (c4) medial views; d, right calcaneum IPS13413 in (d1) medial, (d2) lateral, (d3) posterior, and (d4) distal views; e, left metatarsal IPS866 in (e1) proximal, (e2) anterior, and (e3) posterior views; f, left metatarsal IPS13651 in (f1) distal, (f2) anterior, and (f3) posterior views. Scale bar: 5 cm.

appearance, with its proximodistal diameter being longer than the mediolateral one (Fig. 6b).

Metatarsal—In proximal view, a deep mediolateral furrow divides the anteromedial facet from the posteromedial one, as well as the anterolateral from the posterolateral ones. The lateral articular facets are higher than the medial ones and relatively flat (Fig. 6e). The anteromedial facet has an inverted D-shaped outline, whereas the anterolateral one has a similar, but more complex outline. The posteromedial facet is small and roughly isodiametric; this facet has an irregular outline and is pointed towards the posterior part. There is a large, drop-shaped nutrient foramen in the middle of the proximal epiphysis. The diaphysis is slender (Fig. 6e–f). The anterior part is characterized by the presence of a vascular groove, extending throughout the diaphysis. There is another shallow groove on the

anterolateral border of the proximal shaft. The posterior part of the diaphysis is characterized by the presence of a wide and strong concavity, formed by two longitudinal grooves which disappear toward the distal portion. The distal foramen, located right proximally of the distal epiphysis, has an oval outline. The proximal diaphysis is delimited by two crests, the medial being usually stronger than the lateral. In the distal epiphysis, the sagittal ridges of the trochlea are subparallel in anterior view. In distal view, the two ridges converge anteriorly. The mediolateral diameter of the diaphysis-distal epiphysis margin is slightly greater than that of the trochlear epicondyles.

Astragalus—The astragalus is quite stout, so much so that the width is larger than half of the length (Fig. 6c). The proximal lateral trochlea is higher and wider than the medial one. In anterior view, the intertrochlear notch is wide and smooth and ends distally in a deep, rounded fossa. The distal trochleae are more uniform compared to the proximal ones, although the lateral one is slightly wider. The distal intertrochlear notch is shallower and slightly narrower than the proximal one. The calcaneal articular facet is elongated and subrectangular and it occupies most of the posterior surface of the bone.

Calcaneum—The general appearance of the body is slender with the narrowest part of the posterior surface being right proximal to the sustentacular process (Fig. 6d). The anterior and posterior edges of the calcaneus are slightly convergent towards the proximal end (tuber calcanei), which, when observed from the medial view, forms an almost rounded margin. The cubonavicular facet is smooth, elongated and twisted, changing from a posteromedial orientation in the proximal half to a posterior orientation in the distal half. The anterior process is pointed and it projects distally; in medial view, the process forms a tuberosity with a posteroproximal to anterodistal direction, delimited by a shallow depression. In distal view, the astragalus facet has a subrectangular shape. This facet is also proceeding towards the anteromedial surface of the sustentacular process, with a semicircular outline; it is delimited on the medial margin of the posteromedial sustentacular process by a rough drop-shaped area.

5. Discussion

5.1. Comparisons

5.1.1. Morphological comparisons

Cranium—The cranium from CGR presents a mix of *Cervus*-like and *Dama*-like characters, with the latter ones being prevalent. In fact, the overall shape of the neurocranium is quite spherical, similar to that of the specimen DE 11-1/ind.A from Pirro Nord, attributed to *P. vallonnetensis* (Fig. 7a) (Strani et al., 2024); this character is typical of the modern fallow deer, whereas the red deer shows a more elongated neurocranium. A lengthened neurocranium is also present in some specimens of *P. nestii* such as SABAP_UMB 337643 from Pantalla, IGF243 from Upper Valdarno, and IGF1403 from Olivola, whereas others (e.g., SABAP_UMB 337655 from Pantalla and IGF1404 from Olivola) show a shorter and more rounded neurocranium (Azzaroli, 1992; Cherin et al., 2022). Something similar can be observed, but to a lesser extent, in the Pirro Nord sample referred to *P. vallonnetensis*, where the cranium DE 11-1/ind.B (Fig. 7b) shows a slightly more elongated neurocranium than the aforementioned DE 11-1/ind.A. Similarly, the CGR skull (Fig. 7c) exhibits another *Dama*-like character, which is a high maxilla below the orbit, character also present in the *P. vallonnetensis* specimens from Pirro Nord (DE 11-1/ind.A and DE 11-1/ind.B), as well as in the cranium SABAP_UMB 337643 of *P. nestii* from Pantalla. On the other hand, the skull IGF243 of *P. nestii* from Upper Valdarno shows a *Cervus*-like low maxilla below the orbit. However, it is worth noting that this latter skull belongs to a juvenile individual, hence its morphology should be interpreted with caution. A *Cervus*-like character present in the CGR skull, as well as in the two *P. vallonnetensis* skulls from Pirro Nord is the rather smooth outline of their forehead in lateral view (Fig. 7), that differs from the *Dama*-like steeper

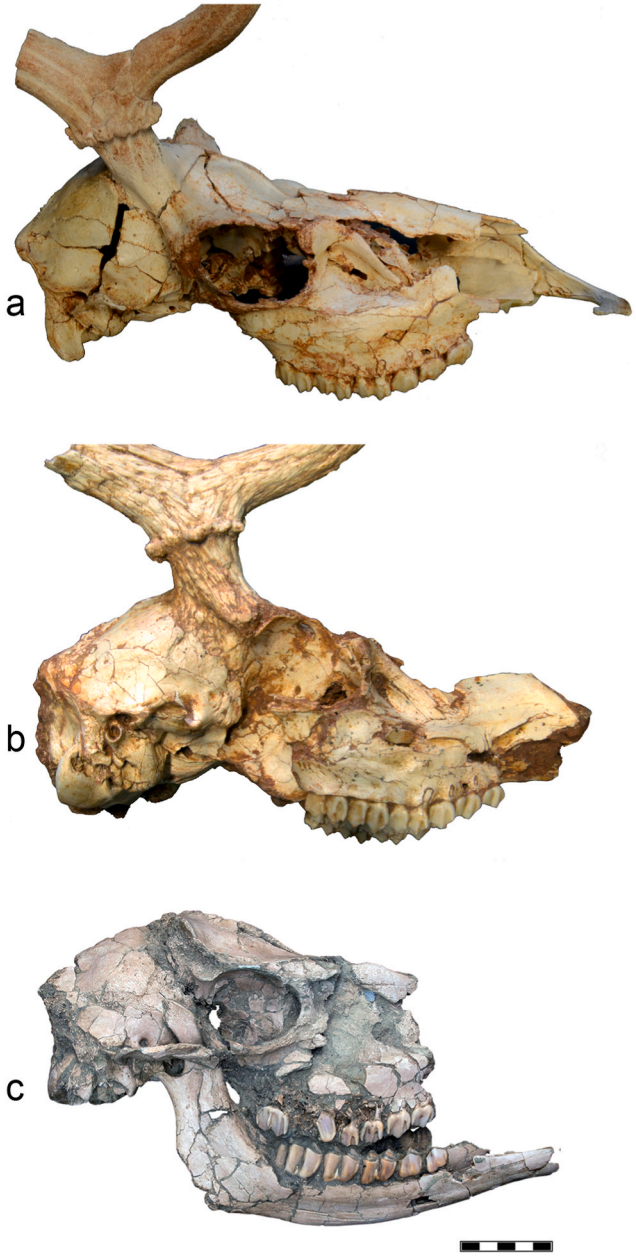

Fig. 7. Comparison of skulls of *Pseudodama vallonnetensis* from Pirro Nord and Cal Guardiola. a, Skull DE 11-1/ind.A from Pirro Nord in right lateral view; b, skull DE 11-1/ind.B from Pirro Nord in right lateral view; c, skull IPS13358 from Cal Guardiola in right lateral view. Scale bar: 5 cm.

forehead, present in the *P. nestii* specimens from Pantalla and Upper Valdarno. The deformation and incompleteness of the CGR skull does not allow further observations on red/fallow deer characters that might be present, such as the muzzle elongation and inclination.

Teeth—The upper molars from CGR show a mix of *Cervus*-like and *Dama*-like characters, with the latter being prevalent. More specifically, some characters are intermediate between the two species (i.e., moderately pronounced columns of buccal cones and styles; Character 1 of Lister, 1996), others are *Dama*-like (i.e., fold present in the mesial wing of the protocone, at least in M2 and M3; weak to moderately developed central lingual column and associated cingulum; weak entostyle and associated cingulum; buccal styles turned horizontally at base to form a shelf; Characters 2–4 of Lister, 1996, respectively), whereas others are *Cervus*-like (i.e., not angled mesiobuccal edge of the tooth near the base; Character 5 of Lister, 1996). In the more primitive

P. nestii from Pantalla, a greater number of upper molar characters (Characters 2–5 of Lister, 1996) scores as *Cervus*-like (Cherin et al., 2022 and personal observations). Interestingly, the mesiobuccal edges of the molars in the specimen IPS13558 show more affinities to *Dama* (i.e., angled), whereas the ones of the specimen IPS14930 to *Cervus* (i.e., not angled). No significant morphological differences between *Dama* and *Cervus* are described in the literature for P2 and P3 (Lister, 1996). The only preserved P4 in CGR belongs to the cranium IPS13558, with only the buccal view visible, where no diagnostic characters are described (Lister, 1996).

Likewise, the CGR lower premolars show mixed characters of *Cervus* and *Dama*. In fact, some characters are intermediate between the two genera (i.e., the entoconid in the lower premolars, having a distolingual direction), others are more similar to *Dama* (i.e., shallow lingual division between entoconid and hypoconid), whereas others are more similar to *Cervus* (i.e., paraconid and parastylid not well separated in the upper part of p3). The lower molars show more *Dama*-like characters (i.e., clear step between second and third lobe of m3 on the lingual side; weak to moderate enamel rugosity; relatively weak lingual columns and furrows in occlusal view; strongly developed mesial buccal cingulum in m1; Characters 11, 8, 4, and 2 of Lister, 1996, respectively). A similar character suite was described for primitive forms of *Pseudodama* such as *P. nestii* from Pantalla (Cherin et al., 2022), except for Character 11 of Lister (1996), which matches the morphology of *Cervus* rather than *Dama* in the Pantalla deer.

Antlers—In most of the specimens from CGR the pedicle is relatively short (average height of 18.6 mm; range: 13.2–26.9 mm; n: 22). Higher pedicles are observed in the slenderest specimens (e.g., IPS16846, in which the height is 26.9 mm), which belong to younger individuals. This inverse relationship between pedicle height and ontogenetic stage (i.e., the pedicles become lower and stockier with aging) is well recognized in the literature for *Dama*-like deer (Breda et al., 2020; Cherin et al., 2022). The relatively low pedicle of (adult) individuals of CGR is a character shared with specimens of *P. vallonnetensis* from Capena, Collecurti, Pirro Nord, Untermassfeld, Atapuerca TD6, and Barranc de la Boella, the *Dama*-like deer from Cueva Victoria (Made, 2015), as well as of *P. farnetensis* from Le Ville-Farneta (type locality) and Casa Palazzi in Val di Chiana (Azzaroli, 1992). The longer pedicle height in juvenile individuals is also reported for *P. vallonnetensis* from Untermassfeld, with a mean value of 31 mm (Breda et al., 2020).

The basal tine of the CGR specimens is always resting on the burr; it emerges almost straight and is oriented slightly outward in its basal part and then it shows a more or less abrupt upward curvature, with a slight inward inclination. This same morphology of the basal tine is visible in adult specimens of *P. vallonnetensis* from Untermassfeld (Breda et al., 2020), Le Vallonnet (de Lumley et al., 1988), Pirro Nord (Petronio et al., 2013; Croitor, 2018), Collecurti and Barranc de la Boella and differs from that of *P. farnetensis* from Le Ville-Farneta and Casa Palazzi, in which the basal tine emerges at a short distance from the burr (Azzaroli, 1992). Similarly, the basal tine of specimen M.P.U.R./M1000 from Capena (Petronio, 1979: Fig. 4) and of the most complete antler from Collecurti (Fig. 8i) is resting on the burr, which forms an angle of about 90° abruptly in its middle part. The partial antler from Nettuno (Italy) attributed to "*Axis eurygonos*" (Mancini et al., 2008) also shows similar characteristics. Conversely, the specimens from Venta Micena and Fuente Nueva 3 have a different morphology, with the basal tine emerging at a distance from the burr (Fig. 8a–d) (Menéndez, 1987; Abbazzi, 2010). This specific morphology, observed in antlers of adult individuals, could suggest a different *Pseudodama* species.

Additionally, all the adult specimens from CGR show a strong basal tine. However, in all the available antlers, irrespective of the ontogenetic stage, the beam is always thicker than the basal tine; this feature is present even in the specimens with the strongest basal tine. This character is also present in *P. vallonnetensis* from Pirro Nord (Fig. 8j–k), Untermassfeld (Breda et al., 2020), Le Vallonnet (Fig. 8l–m), Collecurti (Fig. 8i), Barranc de la Boella (Fig. 8h), Can Jan (Fig. 8g), in the *Dama*-like deer from Cueva Victoria (Made, 2015), Fuente Nueva 3 (Fig. 8a), Cava Redicicoli (Fig. 8e–f) and Nettuno (Mancini et al., 2008: fig. 5d). However, De Lumley et al. (1988) in their differential diagnosis of "*Cervus nestii vallonnetensis*", describe the deer from Le Vallonnet as having the basal tine as thick as the beam throughout the ontogenetic stages.

Furthermore, the antlers from CGR show a variation in the angle formed between the basal tine and the main beam, as this angle can be from slightly acute to obtuse (80–150°), with a mean value of 119° (n: 18) (Supplementary Fig. 1). Similarly, this variation can be observed in *P. vallonnetensis* from Untermassfeld, that measure an angle of 85°–135°, with a mean value of 110° (Breda et al., 2020). This wide-angle range is also noted in other localities. Made et al. (2017) describe a specimen from Atapuerca (Trinchera Dolina) TD8 as forming a wide angle between the beam and the basal tine; in fact, we note that this angle is slightly acute, with an estimated value of almost 85° (Made et al., 2017: fig. 13, image 1). On the other hand, the *Dama*-like deer specimens from Cueva Victoria show a wider angle, reaching a value of 135° (Made, 2015). Those from Capena have an angle of approximately 100° (Petronio, 1979). Both the holotype and paratype of *Cervus nestii vallonnetensis* from Le Vallonnet have an estimated angle of 125° (Breda et al., 2020). The wide angle formed between the main beam and the basal tine is also noted in the *P. farnetensis* specimens from Le Ville-Farneta (IGF194V) and Casa Palazzi (IGF 13962; Azzaroli, 1992).

As mentioned before, although no complete antler is preserved in the CGR record, there are no signs of presence of an intermediate tine, even in the most complete basal portions. This absence of intermediate tine is consistently observed in the *P. vallonnetensis* antlers from Pirro Nord, Untermassfeld, Sima del Elefante, Gran Dolina (both in the Atapuerca complex), and Capena. On the contrary, an intermediate tine is present in the right antler of the holotype of *P. farnetensis* from Le Ville-Farneta (IGF194V) and in both antlers of the better-preserved individual from Casa Palazzi (IGF 13962; Azzaroli, 1992). Another difference between CGR antlers and *P. vallonnetensis* antlers from Untermassfeld, Capena, Pirro Nord on one side, and *P. farnetensis* from Le Ville-Farneta and Casa Palazzi on the other side, seems to be the direction and bending of the main beam. In particular, the antlers of *P. farnetensis* are strongly divergent, with the main beam curving abruptly lateralward in its basal portion (basal to the intermediate tine), becoming almost horizontal (Azzaroli, 1992).

Scapula—Some of the characters listed by Lister (1996) indicate the studied specimens are closely related to *Dama* (Characters 3, 4) while others to *Cervus* (Character 2). Specifically, in the proximal view of specimen IPS13516, the glenoid cavity has a middle flattening of the lateral edge (Character 3). In lateral view, the coracoid tip is not pointed as in *Dama*, but rather squared (Character 2) and the edge between the coracoid process and the glenoid cavity is angled (Character 4). Character 1 seems to be more variable; it scores as *C. elaphus* in specimen IPS13516, as *D. dama* in specimen IPS23423, and it has an intermediate morphology in specimen IPS14974. Therefore, the CGR scapulae have an intermediate morphology between *Dama* and *Cervus*, typical of *Pseudodama*. The variable scoring of Character 1 is also noted in *P. vallonnetensis* specimens from Untermassfeld (Breda, 2015).

Humerus—The specimens from Cal Guardiola display resemblances to those of *P. vallonnetensis* from Pirro Nord (Petronio et al., 2013). The coronoid fossa is deep, creating an antero-posteriorly wide articulation surface, and bearing a short and wide olecranon fossa. The last character is also present in humerus IQW 1982/18271 (Mei. 17791) from Untermassfeld (Kahlke, 1997; Petronio et al., 2013). The relative size of the two pits of the distal epiphysis of the humerus distinguishes *Cervus* from *Dama* (Character 1 in Lister, 1996). The preservation state of most of the humeri of CGR does not allow us to clearly recognize the relative size of the two pits, besides few exceptions, where it seems to be variable. More specifically, in IPS40620B the two pits are of similar size but seem well-divided and thus closer to the *Pseudodama* morphology (Breda, 2015), whereas in IPS13372 the lateral pit is larger than the medial one,

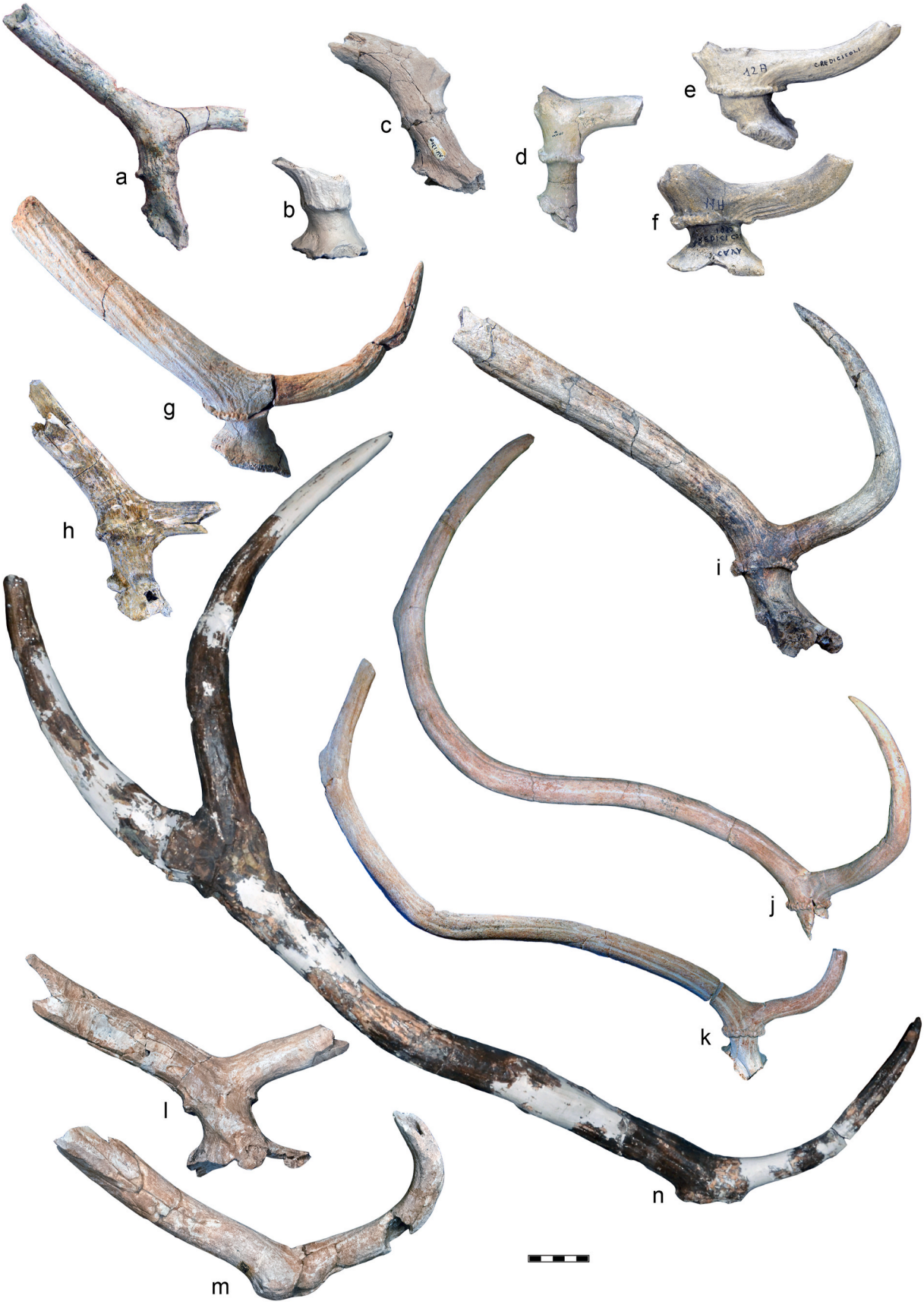

(caption on next page)

Fig. 8. Comparison of antlers of several *Pseudodama* samples from Europe: a, *Pseudodama* gr. *rhenana-perolensis* antler FN3-02-87-UME8 from Fuente Nueva 3, mirrored; b, *Pseudodama* gr. *rhenana-perolensis* antler VM1276 from Venta Micena, mirrored; c, *Pseudodama* gr. *rhenana-perolensis* antler VM1306 from Venta Micena, mirrored; d, *Pseudodama* gr. *rhenana-perolensis* antler VM14 F13 n° 18 from Venta Micena, mirrored; e, *P.* gr. *farnetensis-vallonnetensis* antler 12 A from Cava Redicicoli; f, *P.* gr. *farnetensis-vallonnetensis* antler 11 A from Cava Redicicoli, mirrored; g, *P. vallonnetensis* antler CJ.6 from Can Jan; h, *P. vallonnetensis* antler 2011-K1313 from Barranc de la Boella; i, *P. vallonnetensis* antler n. 179 from Collecurti; j, *P. vallonnetensis* left antler DE 11-1ind.A from Pirro Nord, mirrored; k, *P. vallonnetensis* right antler DE 11-1ind.A from Pirro Nord; *P. vallonnetensis* antler Val, zone B9, couche BJ15, no. 898 from Le Vallonnet; m, holotype of *P. vallonnetensis* Val, zone B7, couche C, n. 10170 from Le Vallonnet; n, *P. vallonnetensis* antler M.P.U.R./M.988 from Capena. Scale bar: 5 cm. Some antlers were mirrored for graphical consistency.

being closer to the morphology of *D. dama* (Lister, 1996).

Radius—The radii of Cal Guardiola exhibit a mix of *Dama* and *Cervus* characters sensu Lister (1996), with the former being more prevalent. In particular, the proximal end of the CGR radii is more similar to fallow deer in the posterolateral margin of the medial glenoid cavity that faces largely anteriorly (Character 1 of Lister, 1996), the relatively indented posterior surface of the main proximal facet (Character 2 of Lister, 1996) and the presence of a sharp pronounced ridge in the posterior surface of the diaphysis, right distally to the proximal epiphysis (Character 7 of Lister, 1996). On the other hand, the proximal end is more similar to red deer in the direction of the lateral tuberosity, that is diagonal in respect to the proximal edge of the radius (Character 5 of Lister, 1996). Character 6 of Lister (1996) seems to be more variable, as in specimens IPS14939 and IPS13225, the posterior edge of the proximal end is moderately raised in respect to the level of the anterior edge, thus resembling *Dama*, whereas, in specimen IPS14991, the level of the posterior edge of the proximal end is strongly raised in respect to the level of the anterior edge, thus resembling *Cervus*. There is a limited number of well-preserved distal ends of radius, however, the two available specimens score differently for the characters of Lister (1996). The distal end of IPS14942 presents a rather convex anterior edge of the medial articular facet and a rather angled posteromedial edge of the same facet (Characters 1, 2 sensu Lister, 1996), resembling *Dama*, whereas specimen IPS13525 presents a less convex anterior edge of the medial articular facet, resembling *Cervus*, and an intermediate state of Character 2, with a relatively smooth, but slightly angled posteromedial edge of the medial articular facet.

Metacarpals—Similarly to other postcranial elements, CGR metacarpals present a mix of red deer and fallow deer characters, with the latter being more prevalent. Although in all available specimens Character 1 of Lister (1996) always scores as *Cervus* (clear space between the medial and lateral facets on the posterior edge of the proximal epiphysis), Characters 3, 4 and 5 score as *Dama* for most specimens, presenting several small slits or pores and a clearly defined mild pit in the medial half of the posterior surface of the diaphysis, right distally of the proximal epiphysis, as well as a rather smooth tuberosity on the medial half of the anterior surface, right distally of the proximal epiphysis. Character 6 (Lister, 1996) can only be clearly observed in specimen IPS16793, presenting a short, mid-sagittal split in the most distal portion of the diaphysis, visible in anterior and posterior view and thus scoring as *Cervus*. The metacarpal of *P. nestii* from Pantalla (SABAP_UMB 337652) scores as *Dama* for Characters 4 and 5 similarly to the CGR specimens, but opposite to the CGR metacarpals, it scores as *Dama* for Character 1 of Lister (1996) (Cherin et al., 2022).

Tibia— The few CGR specimens and their fragmentary state do not allow us to score them according to the characters of Lister (1996). However, specimen IPS39125 scores as *Dama dama* for Character 1 (peaks of the lateral and medial condyle of the proximal epiphysis project almost equally; Lister, 1996), similarly to *P. nestii* specimen SABAP_UMB 167353 from Pantalla (Cherin et al., 2022).

Astragalus—Although Characters 1 and 6 score as *Dama* (edge between the two proximal trochlear ridges is relatively flat and "U" shaped; weak ridge formed in the distolateral border of proximal condyle, in anterior view; Lister, 1996) and Character 5 scores as *Cervus* (pronounced medial bulge in the anterior view, between the proximal and distal condyles; Lister, 1996) in all preserved astragali of CGR, Characters 2–4 present variability across the sample. In particular, specimen IPS13448 (layer CGRD3; 1.2 Ma) scores as *Cervus* for Characters 2, 3 and 4 (steeply inclined medial edge of the lateral tubercle of the proximal trochlea in posterior view; weaker projection of the posterior edge of the medial tubercle of the proximal trochlea; lateral extension of the medial ridge of the proximal end projecting more laterally in its proximal part, rather than in its distal part). Specimen IPS17752 (layer CGRD5; 0.86 Ma) scores as *Dama* for Characters 2 and 3 (moderately steep/gently sloped medial edge of the lateral tubercle of the proximal end in posterior view; stronger projection of the posterior end of the medial tubercle of the proximal trochlea), and has an intermediate morphology between *Dama* and *Cervus* for Character 4 (lateral extension of the medial ridge of the proximal end projects equally in its proximal and distal part). Interestingly, *P. nestii* specimen SABAP_UMB 167353 from Pantalla exhibits similarities to CGR specimens in Character 1 (*Dama*-like morphology; Lister, 1996; Cherin et al., 2022) and Character 5 (*Cervus*-like morphology; Lister, 1996; Cherin et al., 2022). However, it differs in character 6, showing a morphology closer to *Cervus* (Cherin et al., 2022), whereas CGR specimens align more closely with *Dama* in this character. Additionally, Characters 2 and 3 of the Pantalla specimen resemble IPS17752, presenting a *Dama*-like morphology (Cherin et al., 2022), in contrast to the *Cervus*-like morphology of these characters in specimen IPS13448.

Metatarsals—The specimens from Cal Guardiola exhibit a combination of *Cervus* and *Dama* characters, with a notable number of distal portions allowing for the observation of variability in the expression of these traits. In particular, in the proximal view of specimen IPS866 (Fig. 5, a2), Character 1 closely resembles modern fallow deer, as the two large facets of the proximal epiphysis seem to be in contact towards the anterior edge, whereas Character 3 closely aligns with the modern red deer, exhibiting a single, large nutrient foramen (Lister, 1996). The distal ends present variability within the CGR population, since different specimens score either as *Cervus* or *Dama* for the same characters (Characters 4, 5, and 6). More specifically, most specimens (IPS18520, IPS61702, IPS13651, IPS23042) in posterior view exhibit a large and oval-shaped pit/foramen right proximally of the distal epiphysis, scoring as *C. elaphus*, whereas few (IPS18520, IPS13651) exhibit a small and round-shaped foramen (Fig. 5, b3), scoring as *D. dama* (Lister, 1996; character 4). Similarly, variability is noticed in Character 5, as some specimens exhibit a split in the posterior surface of the most distal end of the diaphysis, right proximally to the distal epiphysis (IPS18520, IPS61702), scoring as *C. elaphus*, whereas others (IPS18515, IPS13651, IPS14927) don't exhibit this character, scoring as *D. dama* (Lister, 1996). Finally, variability is also noticed in the expression of character 6 of Lister (1996), as some specimens (IPS18515, IPS61702) present long extensions of the articular surface of the distal epiphysis, similar to *C. elaphus*, whereas others present shorter extensions (IPS18520, IPS14927), similar to *D. dama*. It is also worth noting that no specimen, besides IPS14927 for which all characters of the distal end score as *D. dama*, presents all characters scoring only as *Dama* or *Cervus*. The two metatarsals of *P. nestii* from Pantalla (SABAP_UMB 167353, SABAP_UMB 337651), score as *Dama* for Characters 1–2 and 4–6, thus resembling IPS14927, but differing from all other available distal metatarsal portions from CGR (Cherin et al., 2022).

5.1.2. Biometrical comparisons

The bivariate analyses performed do not show a distinct separation of morphotypes, since there is a linear progression of size change. For

instance, the analysis of the total versus articular (trochlear) transversal diameter of the distal epiphysis of the humerus (Fig. 9a) shows that *P. perolensis* and *D. dama* have the smallest values of all the analyzed samples; *P. rhenana*, *P. nestii*, and *P. vallonnetensis* have overlapping ranges, however, the dimensions of *P. vallonnetensis* and *P. rhenana* tend to be larger than those of *P. nestii*. The humeri from CGR fall exactly in the middle of the range of *P. vallonnetensis*, and in the mid-lower part of that of *P. rhenana*.

The violin plot analysis of the articular (trochlear) transversal diameter of the distal epiphysis of the humerus is more informative: the different records are organized along the vertical axis in chronological order (Fig. 9d). This measurement decreases from *P. rhenana* to *P. perolensis* and increases from the latter to *P. vallonnetensis*. CGR specimens' dimensions almost completely overlap with those of *P. vallonnetensis*. As a matter of fact, the mean value recorded in CGR specimens is the greatest among the available data. There is a gradual tendency of shortening of this variable from *P. vallonnetensis* and CGR, to *D. roberti* and extant *D. dama*.

The graph of the distal anteroposterior versus transversal diameters of the metacarpal (Fig. 9b) shows that extant *D. dama* have the smallest epiphyses compared to the other analyzed samples. *Pseudodama nestii* and *P. vallonnetensis* form the two largest, almost non-overlapped ranges, with *P. farnetensis* from the locality of Selvella-Gioiella placed in between. The only available specimen from CGR falls very close to the *P. vallonnetensis* range. The three available distal metacarpals of *D. clactoniana* (sites of Vitinia, Tor di Quinto, and Riano) encompass a dimensional range included between the middle parts of those of *P. nestii* and *P. vallonnetensis*.

No complete metatarsals of adult individuals are preserved in CGR. The bivariate analyses of the distal epiphyses of the metatarsals (Fig. 9c) show a pattern similar to that described above for the metacarpal. *Dama dama*, *P. nestii*, and *P. vallonnetensis* are arranged in the graph according to the increasing size of the metatarsal, though with some overlapping. CGR specimens fall between the ranges of *P. nestii* and *P. vallonnetensis*.

5.2. Taxonomical assignment of the studied specimens

The taxonomy of Plio-Pleistocene cervids has been traditionally based on antler, but, in recent years, cranial, and dental morphological characters, as well as general body size have been repeatedly taken into account (e.g., Pfeiffer, 2005; Croitor, 2006; Breda et al., 2020; Cherin et al., 2022; Strani et al., 2024). The overall morphology and dimensions of CGR specimens allow their unambiguous attribution to the *Pseudodama* group. Although showing a mosaic of *Dama*-like and *Cervus*-like dental and postcranial characters, exhibiting also intraspecific variability in some cases for the postcranial remains (e.g., distal end of metatarsals), the former are prevalent in the deer from CGR, supporting a closer affinity with the fallow deer, as evidenced for other samples of derived forms of *Pseudodama* (e.g., *P. vallonnetensis* from Untermassfeld). On the contrary, earlier species of the genus such us *P. nestii* show a greater number of *Cervus*-like anatomical characters. The position of the basal tine resting on the burr, the obtuse angle it forms with the main beam, the rather straight and not strongly lateralward curving basal beam portions, the lack of evidence of any intermediate tine or palmation in the CGR antlers are characters present in all *P. vallonnetensis* samples. Although sufficiently complete comparative material is scanty, the cranium and mandible of the CGR deer share several similarities with the samples from Pirro Nord and Untermassfeld, both referred to *P. vallonnetensis*. The size of the analyzed postcranial bones is always in the ranges of the same species. Based on the above characters, the CGR sample is confidently referred to *P. vallonnetensis*.

5.3. Biochronological significance of Pseudodama vallonnetensis in the European context

Based on earlier studies of the Vallparadís Section and this first comprehensive examination of fallow deer remains across all layers of the Cal Guardiola section, the species *P. vallonnetensis* is identified within the Vallparadís Section during the chronological interval spanning from 1.2 to 0.86 Ma (MIS 35–21; Madurell-Malapeira et al., 2010, 2012, 2017). This species is also reported in other late Early Pleistocene sites in Iberia, including Sima del Elefante TE9, Trinchera Dolina TD4-6, El Penal, Barranc de la Boella, and Can Jan (Incarcal Complex) (Made, 1999; Madurell-Malapeira et al., 2019), all within the same chronological span. Other records from the Iberian Peninsula such as Cueva Victoria and Cueva Negra del Estrecho del Río Quipar might be referred to the same taxon as well (Walker et al., 2020; Made, 2015), but the evidence available to date does not allow us to confirm this with certainty. Indeed, the spread of *P. vallonnetensis* in Iberia at ca. 1.2 Ma, alongside *Megaloceros savini* and *Bison schoetensacki*, corresponds to the beginning of the Epivillafranchian biochron (Madurell-Malapeira et al., 2019; Sorbelli et al., 2021).

However, earlier (i.e., latest Villafranchian) sites in Iberia such as Venta Micena, Barranco León-D, Fuente Nueva 3, and Alto de las Picarazas, would document a more primitive form of *Dama*-like deer, which is reported in the literature as *P. rhenana* (Abbazzi, 2010; Gabarda et al., 2016; Martínez-Navarro et al., 2018).

The situation in France remains less clear, primarily due to the limited availability of chronologically well-constrained sites. *Pseudodama rhenana* is well documented in some Middle and probably early Late Villafranchian sites such as Saint-Vallier and Senèze (Palombo and Valli, 2003, Pfeiffer-Deml, 2016). The later species *P. perolensis* is enigmatic. It is known with certainty only from the type locality of Peyrolles (late Late Villafranchian; ca. 1.5 Ma) with numerous remains but not complete antlers (Bout and Azzaroli, 1952; Heintz, 1970; Valli et al., 2006). According to Vos et al. (1995), the species is a junior synonym of *P. rhenana*, but there is no consensus on that (e.g., Valli et al., 2006; Breda and Lister, 2013; Cherin et al., 2022), whereas Palombo and Valli (2003) refer to it as a subspecies of *P. rhenana*, reporting the taxon in the type locality of Peyrolles, as well as the localities of Blassac la Girondie and possibly Durfort. In the Epivillafranchian, akin to Iberia, *P. vallonnetensis* is identified in its type locality at Le Vallonnet (ca. 1.2–1.1 Ma; de Lumley et al., 1988; Moullé, 1992; Moullé et al., 2006; Michel et al., 2017). Since the taxonomical status of *P. perolensis* is still debated and a revision of all Late Villafranchian medium-sized cervids is outside the scope of this paper, we are cautiously referring to the fragmentary Iberian samples from Venta Micena, Barranco León-D, Fuente Nueva 3 and Alto de lad Picarazas as *Pseudodama* gr. *rhenana-perolensis*, pending an in-depth assessment of the species' systematics.

The fossil record of the Late Villafranchian and Epivillafranchian of Northern and Central Europe is quite scarce. During the Late Villafranchian, *P. rhenana* is recorded in Tegelen, The Netherlands, and dubiously in East Runton, UK (Cherin et al., 2022 and references therein), whereas *P. vallonnetensis* is recorded in the Epivillafranchian site of Untermassfeld (ca. 1.0 Ma; Breda et al., 2020). The latter is one of the key-reference sites for the Epivillafranchian period, and it stands out for the richness and preservation status of its faunal assemblage (Kahlke, 2009 amongst others), as well as the large collection of *P. vallonnetensis* remains, whose studies were seminal in shaping the current knowledge of the taxon (Kahlke, 1997, 2001; Breda et al., 2020). The presence of the species indicates that *P. vallonnetensis* was also widespread in Central Europe during the Epivillafranchian.

The Italian record is particularly rich and allows to fill some chronological gaps. The early species *P. rhenana* is not well represented, being only reported with scanty remains in very few late Middle Villafranchian sites such as Coste San Giacomo and Cava Toppetti (Cherin et al., 2022). In the early Late Villafranchian, *P. nestii* is widespread, especially in central Italy (Azzaroli, 1992). *Pseudodama nestii* is followed by *P. farnetensis* in some late Late Villafranchian sites (Azzaroli, 1992; Cherin et al., 2022), marking the transition (alongside other faunal changes) between the Tasso Faunal Unit and the Farneta Faunal Unit in

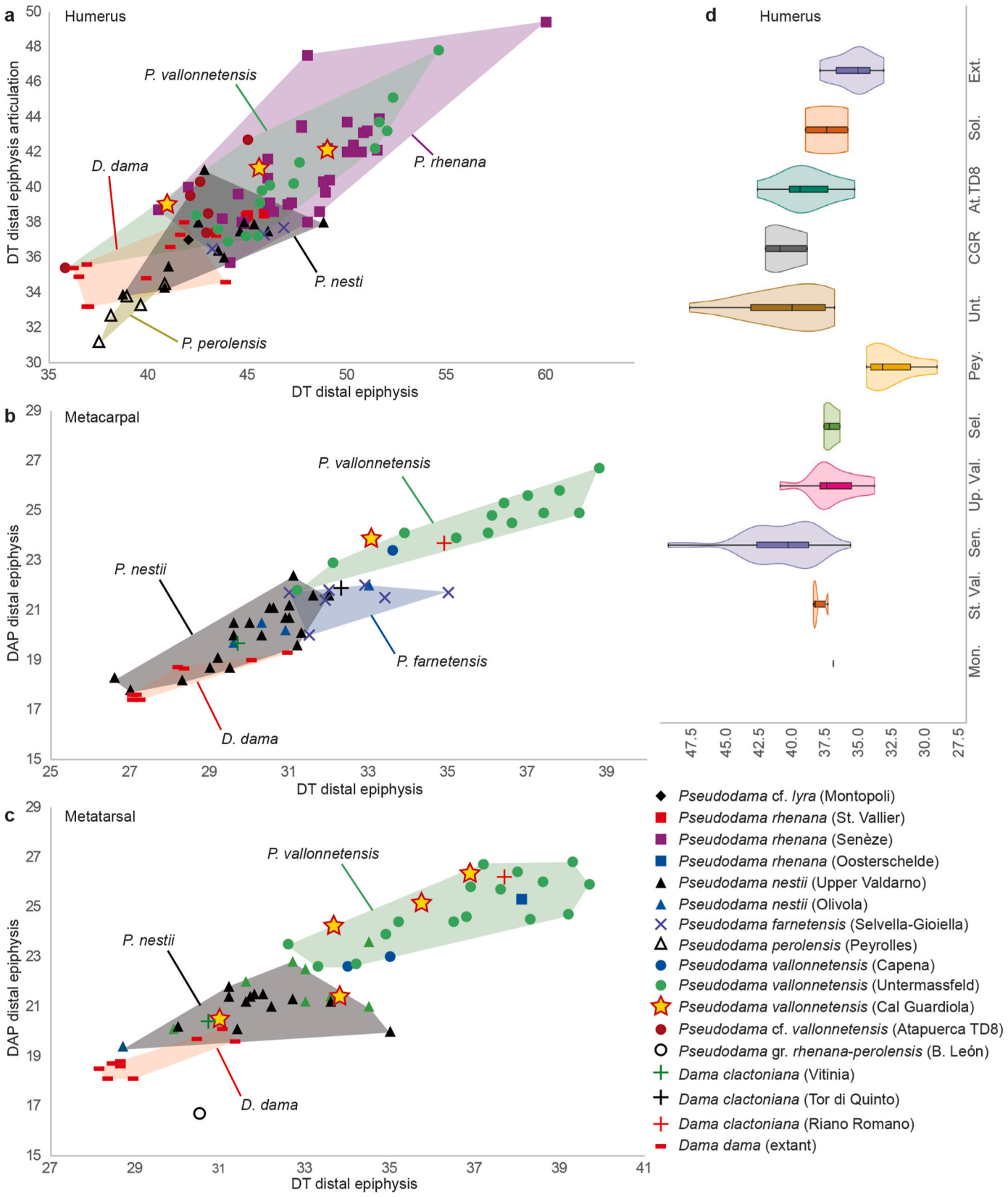

Fig. 9. Biometrical comparisons of limb bone dimensions of several *Dama* and *Dama*-like deer species; a, bivariate plot of the total transversal diameter and the articular (trochlear) diameter of the distal end of humerus; b, bivariate plot of the transversal and anteroposterior diameters of the distal epiphysis of metacarpals; c, bivariate plot of the transversal and anteroposterior diameters of the distal epiphysis of metatarsals; d, violin plot of transversal diameter of the distal epiphysis articulation of humerus. All measurements are in mm. Abbreviations: At. TD8, Atapuerca Complex (Trinchera Dolina TD8); CGR, Cal Guardiola; Ext., extant *Dama dama* from the Iberian Peninsula; Mon., Montopoli; Pey., Peyrolles; Sel., Selvella-Gioiella; Sen., Senèze; Sol., Soleilhac; St. Val., Saint Vallier; Unt., Untermassfeld; Up. Val., Upper Valdarno.

the Italian large-mammal-based biochronological framework (Gliozzi et al., 1997). Conversely, the replacement of *P. farnetensis* by *P. vallonnetensis* is subtler, as the two species share many characters of the antlers and a similar body size. In addition, no complete skulls of *P. farnetensis* are known to date. Especially around the Villafranchian-Epivillafranchian transition, numerous fragmentary records (e.g., Redicicoli, Monte Peglia, Frantoio) should be cautiously referred to *P.* gr. *farnetensis-vallonnetensis*. Nevertheless, latest Villafranchian sites such as Pirro Nord and Capena, yielded a form of fallow deer entirely comparable to *P. vallonnetensis* (*Dama vallonnetensis* in Croitor, 2014, 2018), yet referred to different taxa by some other authors (Petronio, 1979; De Giuli et al., 1986; Petronio et al., 2011, 2013). Unfortunately, no precise dating of the aforementioned sites is available to date. Biochronological data point towards an age range of ca. 1.6 to 1.3 Ma for Pirro Nord (Arzarello et al., 2012; Pavia et al., 2012; Lopez-Garcia et al., 2015), and the poor assemblage from Capena might have a similar age (Cherin et al., 2022). It is worth noting that some recent geochronological analyses would suggest a younger age for some Pirro Nord sites (Duval et al., 2024), although the same results should be taken with caution considering possible sedimentological biases and/or a complex formation history of the fossiliferous deposit at the site (Duval et al., 2024). Pending conclusive chronological data on these Italian sites, their records suggest the occurrence of *P. vallonnetensis* already soon before or at the very beginning of the EMPT. The *P. vallonnetensis* record from Collecurti (ca. 1 Ma; Madurell-Malapeira, 2022) demonstrates the unequivocal presence of the species in Italy in the middle of the Epivillafranchian stage.

Finally, the Greek record is notably more limited. The Middle and possibly the early Late Villafranchian is characterized by the presence of *P. rhenana* (sites of Volax, Dafnero, Sesklo, Vatera among others; Kostopoulos, 1997; Vos et al., 2002; Kostopoulos and Athanassiou, 2005). Remains from the Late Villafranchian locality of Libakos, initially described as *C. nestii eurygonos* (Steensma, 1988) and recently referred to the species *Dama vallonnetensis* (Athanassiou, 2022), are here included in *P. vallonnetensis*. However, the absence of well-preserved remains from the late Late Villafranchian and Epivillafranchian prevents a clear reconstruction of the evolutionary history of this group of cervids in the area (Koufos and Kostopoulos, 2016). According to the recent biochronological assessment of Greek large mammal assemblages by Konidaris and Kostopoulos (2024), derived forms of *Dama*-like deer (probably attributable to what we refer to *P. vallonnetensis* in the present study) replaced earlier *Pseudodama* forms in the Krimni Greek Faunal Unit (centered around 1.6–1.5 Ma).

The above pieces of evidence suggest the intriguing possibility that *P. vallonnetensis* may have spread to Greece and then to Italy before the rest of southern Europe (i.e., already in the latest Villafranchian, through an east to west dispersal).

5.4. Body size estimations in Dama-like deer

Some interesting inferences can be made by observing the variations in body size of *Dama*-like deer over time, reconstructed using m3 width as a proxy of body mass (Fig. 10). The body mass estimated for the available fossils from Montopoli, Italy (Plio-Pleistocene boundary) is approximately 110 kg. In the rest of the Middle Villafranchian (French sites of Saint Vallier and Senèze) and earliest Late Villafranchian (Italian site of Pantalla), the body mass remains lower than that observed in Montopoli, but a continuous increasing trend of the mean value is

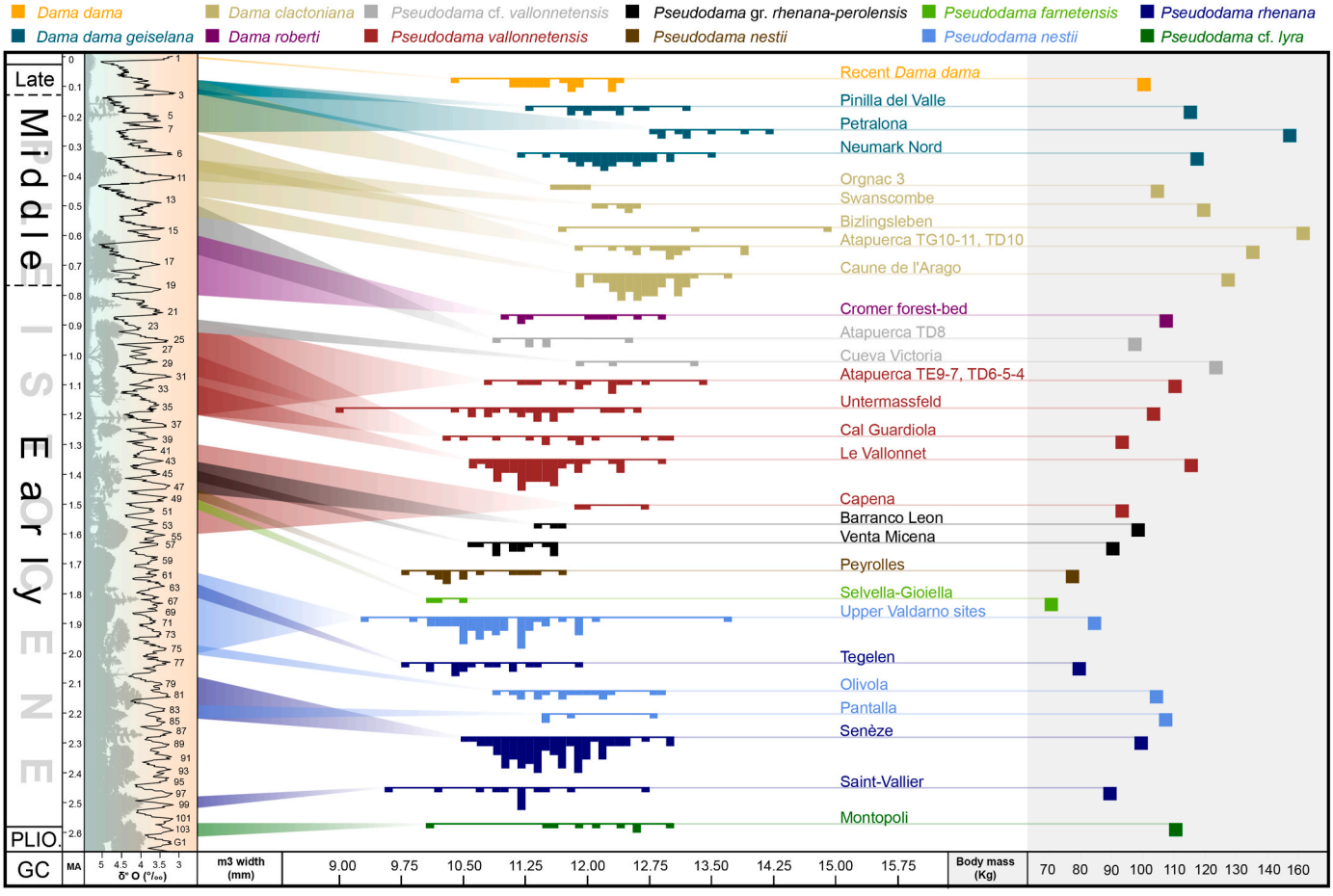

Fig. 10. Jitter plot of the m3 width variation of selected *Dama* and *Dama*-like deer Quaternary samples and mean estimated body mass. Measurements as in Supplementary Table 3. Cromer Forest Bed* refers to Cromer forest bed Formation in Pakefield and West Runton.

observed, culminating in a peak at Pantalla (107 kg). This peak is followed by a decrease of body mass of *Dama*-like deer after ca. 2.0 Ma, in the localities of Olivola (104 kg) and especially Tegelen (79 kg). Conversely, in the ca. 1.8–0.8 Ma time interval (Late Villafranchian and Epivillafranchian), the mean body mass of *Dama*-like deer gradually increases, with the samples from Sima del Elefante TE9-7 and Trinchera Dolina TD6-5-4 reaching the maximum value of this period (110 kg). Interestingly, during the Epivillafranchian, we note a generally higher mean body mass than in the Late Villafranchian, with very slight fluctuations (93–109 kg). The body mass estimation of the fallow deer from Cueva Victoria (123 kg) should be interpreted with caution due to the small sample size (three measurements). During the Middle and Late Pleistocene, more fluctuations in average body mass are detected, with maximum values reached in Galería Complex TG10-11 and Trinchera Dolina TD10 (135 kg) and especially Petralona, Greece (147 kg) and Bizlingsleben (151 kg), however, the very small sample size of the latter site should urge caution when considering the results. Nevertheless, the body mass of *Dama*-like deer stands at high values (>95 kg) throughout this period (Atapuerca TD8, Spain: 97 kg; Cromer Forest-bed Formation at Pakefield and West Runton, UK: 107 kg; Caune de l'Arago, France: 127 kg; Swanscombe, UK: 119 kg; Orgnac 3, France: 104 kg; Neumark Nord, Germany: 117 kg; Pinilla del Valle, Spain: 115 kg). Finally, the recent populations of *D. dama* seem to have a decreased body mass compared to the Late Pleistocene fallow deer, however similar to that of the Epivillafranchian forms (ca. 100 kg).

The body mass fluctuations detected along the evolutionary history of *Dama*-like deer in Pleistocene Europe might depend on a wide array of factors, including climate and specifically, temperature (e.g., Bergmann's rule), habitat openness, resource availability, faunal composition of the assemblage (e.g., predatory pressure, interspecific competition), geographic isolation (e.g., island rule), and finally, phylogenetic trends. Having built Fig. 10 without a priori taxonomic information, but organizing the *Dama*-like deer samples only according to the age of the sites of provenance, allowed us to exclude any taxonomic bias. Based on our results, the body mass of *Dama*-like deer does not seem to strictly depend on the climatic conditions of each habitat. For example, the early Late Villafranchian samples from Olivola and Pantalla show a similar mean body mass estimation (104 and 107 kg, respectively), although the paleoenvironmental conditions in the two sites were completely different; in fact, the paleoenvironment of Olivola can be characterized as mostly open, due to the predominant presence of open grasslands and the scattered presence of thickets and open woodlands (Strani et al., 2018), as opposed to the closed paleoenvironment of Pantalla, that was mainly characterized by the presence of a conifer dominated forest (Cherin et al., 2023). In addition, the obtained body mass values do not seem to be affected by the latitude of the sites that the different populations inhabited. In fact, we note that during the Epivillafranchian, the several populations of *P. vallonnetensis* attained very similar body mass values (93–110 kg) throughout Southern, Western, and Central Europe, with the largest mean value being attained in the Iberian site complex of Atapuerca (TE9-7, TD6-5-4) (Fig. 10), in accordance with the results of Made et al. (2017: fig. 15). Obtaining the largest body mass estimate for the sample from the southernmost Epivillafranchian site is noteworthy, as it is in disagreement with what would be expected according to the Bergmann's rule. As further proof, it is interesting to note that the body mass (93 kg) estimated for the Untermassfeld *Dama*-like deer, which lived in the super-interglacial period of MIS 31 (based on magnetostratigraphic and biostratigraphic evidence; Kahlke, 2022 and references therein) is exactly the same as the one estimated for the sample from Le Vallonnet, which corresponds to a glacial period (based on palynological analyses; Renault-Miskovsky and Girard, 1978; Cauche, 2022). This observation further challenges the validity of Bergmann's rule for this group of animals. Interestingly, Stefanelli and Mecozzi (2020) suggested that Middle Pleistocene *Dama*-like deer exhibited larger body mass during interglacial periods, due to increased resource availability. Most Middle Pleistocene samples we addressed in our analysis (e.g., Cromer Forest-bed Formation at Pakefield and West Runton; Swanscombe; Neumark Nord) come from interglacial periods (Schreve, 2001; Breda and Lister, 2013; Kindler et al., 2020; Laurat and Brühl, 2021 and references therein), thus we cannot furtherly test the results of Stefanelli and Mecozzi (2020). The lack of absolute dating or paleobotanical data in older sites is another restrictive factor in addressing the relationship of body mass to mean temperature (i.e., glacial/interglacial fluctuations). Based on the available evidence, there does not appear to be a direct correlation between climate and body size in *Dama*-like deer, at least during the Epivillafranchian, since all the examined samples show a stable body mass regardless of latitude and paleoenvironmental conditions. Another logical argument is that overcrowded ungulate assemblages would increase intergeneric resource competition, resulting in lower body size, as seen for example in the case of Venta Micena. However, studies like that of Filella et al. (2024) have demonstrated that extant fallow deer can adapt their feeding behavior to the presence of other sympatric genera with the same or similar dietary preferences (e.g., bison) and can even take better advantage of high-quality resources. The investigation of the influence of other possible factors, such as the faunal composition of the assemblage and predation, on the body mass of all the European *Dama*-like deer is beyond the scopes of this study.

Summarizing the above results and integrating taxonomic information (Fig. 10), it seems that the primary factor influencing the body mass fluctuations of *Dama*-like deer is taxonomy, meaning that different species had different size ranges. It is likely that other factors, such as paleoclimate, may also affect body mass within the same species. In fact, body size differences among *Dama*-like deer species, particularly *Pseudodama* species, based on their limb bone proportions, were already noted by Azzaroli (1992). According to this last author, *P. nestii* had a slightly smaller body size than *P.* cf. *lyra* from Montopoli, and *P. farnetensis* had a smaller size than *P. rhenana* from Senèze and *P.* cf. l*yra* from Montopoli. Indeed, our body mass estimation analysis reveals the same differences in body mass. Further studies considering all the aforementioned factors and their interactions could clarify the driving forces behind the body mass evolution of the group during the Quaternary.

5.5. Paleoenvironmental significance of *P. vallonnetensis*

The extant fallow deer *D. dama* displays an exceptionally broad spectrum of food preferences and diet plasticity based on resource availability. Consequently, the current distribution of this species, native to Europe and the Near East, spans various habitats and regions in Eurasia, Africa, the Americas, and several other areas in which it was introduced by humans (Esattore et al., 2022). On the other hand, information on the ecology of *Pseudodama* species is limited, due to the scarcity of dedicated studies and the lack of paleoenvironmental data from many of the paleontological localities in which they were recovered.

The scenario in the late Early Pleistocene of the Iberian Peninsula seems heterogeneous in time. In many Late Villafranchian sites such as Venta Micena, Alto de las Picarazas, or Fuente Nueva 3, *Dama*-like deer are not as abundant as grazer/mixed-feeder bovids like *Praeovibos, Soergelia*, *Hemitragus, Ammotragus, Eobison* or *Hemibos*. The paleoenvironmental conditions between 1.6 and 1.2 Ma in Iberia were characterized by open woodlands and savannas, with predominant arid conditions during the 1.6–1.4 Ma interval (Saarinen et al., 2021). As the EMPT intensified around 1.2 Ma (Head and Gibbard, 2015), environmental conditions in Iberia shifted to more closed woodlands, accompanied by increased humidity, seasonality, and precipitation (Fidalgo et al., 2023). This transition is exemplified by the wood and pollen analysis of layer CGRD2, indicating warm-temperate and humid conditions suggestive of a river or river-marsh ecosystem (Mijarra et al., 2007). This period roughly coincided with the initial records of *P. vallonnetensis*, which became predominant in the fossil assemblages of the Vallparadís Section across all layers, alongside *Hippopotamus*

antiquus (Madurell-Malapeira, 2023). Subsequently, during MIS 30, an arid period is documented (Strani et al., 2019; Sorbelli et al., 2021; Fidalgo et al., 2023; Madurell-Malapeira, 2023). In layer EVT12 of the Vallparadís Section, *Hippopotamus* is very rare and *P. vallonnetensis* emerges as the dominant species, exhibiting predominantly grazing habits (Strani et al., 2019). Finally, in layers CGRD7 and EVT7 during MIS 21, *Hippopotamus* and *Pseudodama* are once again the most documented species, with the latter shifting to a mixed-feeding behavior (Strani et al., 2019; Madurell-Malapeira, 2023; Vizcaíno-Varo, 2023). It is interesting to highlight that, like *Pseudodama*, Early Pleistocene hippos also demonstrate a high degree of resilience and ecomorphotypic adaptability (Fidalgo et al., 2023).

The situation in France appears similar to that in the Iberian Peninsula. Savanna-like landscapes, but less arid than in Iberia, are recorded in the 1.6–1.2 Ma interval. Similarly, an increase in humidity, seasonality, and climatic asymmetry is reported since 1.2 Ma, coinciding with the first records of *P. vallonnetensis* (Renault-Miskovsky and Girard, 1978; Renault-Miskovsky and Lebreton, 2006; Leroy et al., 2011). In terms of tree taxa, the EMPT in southern France and northeastern Spain is marked by the spread of *Quercus*, *Picea*, *Abies*, *Carpinus*, and increasing *Fagus* (Magri et al., 2017).

In Italy, during the second half of the Early Pleistocene, the distribution and diversity of plant taxa exhibit several differences compared to France and Iberia (Bertini, 2010; Bertini et al., 2010; Magri and Palombo, 2013). Various taxa, such as *Pterocarya, Tsuga, Cedrus*, and *Zelkova*, were more abundant in Italy than in France and Iberia (Magri et al., 2017). On the contrary, the overall increase in open vegetation observed in France and Iberia since 1.5 Ma was less pronounced in Italy, but still significant especially in the central and southern areas of the country (Magri and Palombo, 2013; Magri et al., 2017). Between 1.5 and 1.2 Ma, while *P. rhenana* or a related form that in this paper we refer to as *P.* gr. *rhenana-perolensis* inhabited moderately open spaces in France and Iberia, the prevalence of wood cover in Italy likely facilitated the first records of *P. farnetensis* followed by *P. vallonnetensis*. Records of *Dama*-like deer are scanty in the latest Villafranchian, but the few data available seem to indicate that the typical species of this period, namely *P. farnetensis*, lived in environments characterized by forests in which *Carya* and *Tsuga* were the dominant trees, followed by *Pinus*, *Cedrus*, *Picea*, and *Quercus*, at least in central Italy (Magri et al., 2017). *Pseudodama vallonnetensis* is first recorded in Italy at Pirro Nord (ca. 1.6–13 Ma; Petronio et al., 2013; Croitor, 2014, 2018). Regardless of the uncertainties on the age of the assemblage (Duval et al., 2024), all available data agree on the recognition at Pirro Nord of an open environment with patches of woodland in locally wetter areas (Bedetti and Pavia, 2013; Blain et al., 2019; Strani et al., 2024). In this conditions, *P. vallonnetensis* exhibits a long-term mixed diet with a tendency towards grazing at Pirro Nord (Strani et al., 2024), similarly to what is observed in the aforementioned layer EVT12 of the Vallparadís Section, also documenting an arid phase (Strani et al., 2019). Further preliminary geochemical analysis confirms a mixed-feeding diet for the fallow deer from Pirro Nord when compared with taxa with a higher tendency towards grazing such as bovids, rhinos and horses from the same site (Ramada, 2024). In another Italian site where *P. vallonnetensis* is reported, namely Collecurti (ca. 1 Ma), paleoenvironmental information points towards greater heterogeneity over time. Palynological data show alternations between relatively warm and humid phases (interglacials) dominated by montane coniferous forests with *Tsuga*, *Abies*, *Picea*, and *Pinus*, and relatively cold and dry phases (glacials) dominated by Chenopodiaceae and *Artemisia* (Coltorti et al., 1998; Bertini, 2000). The Collecurti bonebed is largely dominated by *Hippopotamus*, being suggestive of wet climate with mild winter temperatures, but it is immediately overlaid by a stratigraphic interval indicating a dramatic change toward a colder and drier phase (Mazza and Ventra, 2011). Consequently, this information does not allow to precisely associate the presence of *P. vallonnetensis* with a specific paleoenvironment, but suggests a certain difference compared to what is observed at Pirro Nord. The paleoenvironmental context in which the Collecurti bonebed accumulated, might be similar to what is observed in the hippopotamus-dominated layers of the Vallparadís Section (see above). Therefore, the combined inferences between the Vallparadís Section, Pirro Nord and Collecurti support a certain ecological plasticity of *P. vallonnetensis* (Strani et al., 2019, 2024; Vizcaíno-Varo, 2023; Ramada, 2024).

A mixed feeding behavior was hypothesized based on craniodental anatomy also for *P. vallonnetensis* from Untermassfeld (ca. 1 Ma; Breda et al., 2020). Unfortunately, no quantitative proxies (e.g., dental wear or stable isotope data) are available for the Untermassfeld deer sample to corroborate this hypothesis. Herpetological data strongly indicate the widespread presence of warm, dry open areas in the region, associated with scattered seasonal or perennial water bodies (Böhme, 2020), that is, a context not much dissimilar than that described in Pirro Nord (see above).

6. Conclusions

The specimens of *Dama*-like deer from Cal Guardiola exhibit numerous similarities with those from the German site of Untermassfeld, where both juvenile and adult specimens have been documented, and the smaller sample from Le Vallonnet, type locality of *P. vallonnetensis* (de Lumley et al., 1988; Moullé, 1990; Breda et al., 2020). Through the decades, several Early Pleistocene *Dama*-like deer specimens were assigned to different genera and species, creating a confusing taxonomy for this group (e.g., Di Stefano and Petronio, 1998, 2002; Croitor, 2018). However, we suggest that records such as those of Sima del Elefante TE9 and Trinchera Dolina TD6, Barranc de la Boella, Can Jan (Madurell-Malapeira, 2022), Pirro Nord, and Collecurti encompass the morphological variability observed in both the Cal Guardiola and Untermassfeld samples. We propose that the absence of juvenile material and complete antlers of *P. vallonnetensis* from its type locality may have led to biased assumptions included in the species' diagnosis. The examination of material from different ontogenetic stages, as studied and described primarily at Untermassfeld (Breda et al., 2020) and in the present work, could represent the initial step toward a more accurate reconstruction of the species' morphology throughout various stages of its life.

The paleobiogeographic distribution of *Dama*-like deer in Europe during the late Early Pleistocene reveals several intriguing insights. *Pseudodama vallonnetensis* was a common faunal element during the Epivillafranchian biochron (ca. 1.2–0.8 Ma) in Southern, Western, and Central Europe, demonstrating a remarkable ability to disperse across various latitudinal zones. The species replaced *P. rhenana* and possibly *P. perolensis* or other related forms in France and the Iberian Peninsula (ca. 1.2–1.1 Ma), *P. rhenana* in Greece (ca. 1.6–1.5 Ma), and *P. farnetensis* in Italy during the latest Villafranchian (e.g., Pirro Nord, Capena). The exact dating of this last replacement is unclear, due to the fragmentary nature of the *Dama*-like deer remains from the Villafranchian-Epivillafranchian boundary (e.g., Cava Redicicoli, Monte Peglia, Frantoio), which we hereby cautiously refer to *P.* gr. *farnetensis-vallonnetensis*. The advent of *P. vallonnetensis* sensu stricto in Iberia is recorded at the onset of the Epivillafranchian biochron around 1.2 Ma, and slightly later (ca. 1.0 Ma) in Germany (although in this area the absence of paleontological sites chronologically preceding Untermassfeld should be emphasized). The enthralling possibility of an east to west dispersal of the species is suggested by its possible presence in Italy and Greece already during the latest Villafranchian (ca. 1.6–1.3 Ma), though this hypothesis remains to be tested. Climatic changes such as increase of humidity and seasonality accompanied by a spread of *Quercus* and *Picea* forested environments in Iberia and France at the beginning of the EMPT, seem to have favored further dispersal of *P. vallonnetensis* towards the west.

Climate changes throughout the Quaternary and/or local environmental conditions do not appear to be the main factors driving the

differences in body mass estimated for European Quaternary *Dama*-like deer, similarly to what has been proposed in previous works (e.g., Made et al., 2014; Made et al., 2017; Stefanelli and Mecozzi, 2020). Our results suggest that the body mass changes are mainly taxon related (i.e., different size ranges for different species) and not primarily related to climatic factors, further endorsing Azzaroli's (1992) conclusions at least for *Pseudodama* species.

CRediT authorship contribution statement

Elpiniki-Maria Parparousi: Writing – review & editing, Writing – original draft, Visualization, Methodology, Investigation, Funding acquisition, Formal analysis, Data curation, Conceptualization. **Leonardo Sorbelli:** Writing – review & editing, Visualization, Investigation, Funding acquisition, Formal analysis. **Marco Cherin:** Writing – review & editing, Writing – original draft, Supervision, Project administration, Methodology, Investigation, Conceptualization. **Marzia Breda:** Writing – review & editing, Writing – original draft, Supervision, Investigation, Funding acquisition, Conceptualization. **Alessandro Blasetti:** Resources. **Marco Peter Ferretti:** Writing – review & editing, Resources. **Darío Fidalgo:** Writing – review & editing, Resources. **Saverio Bartolini-Lucenti:** Writing – review & editing, Resources, Funding acquisition. **Pierre-Élie Moullé:** Resources. **Bienvenido Martínez-Navarro:** Writing – review & editing, Resources, Funding acquisition. **Lorenzo Rook:** Resources. **Joan Madurell-Malapeira:** Writing – review & editing, Writing – original draft, Resources, Investigation, Funding acquisition, Conceptualization.

Declaration of competing interest

The authors declare that they have no known competing financial interests or personal relationships that could have appeared to influence the work reported in this paper.

Acknowledgments

Research on the Vallparadís Section has been funded by the Departament de Cultura de la Generalitat de Catalunya under the research project '*Evolució dels ecosistemes dels Pirineus Orientals i àrees adjacents durant el Pleistocè: 2022–2025*' of which J.M.-M. is the principal investigator. E.-M.P.'s PhD is funded by Next Generation EU through PNRR, mission 4, component 1 ("Potenziamento dell'offerta dei servizi di istruzione: dagli asili nido all'università"), investment 3.4 ("didattica e competenze universitarie avanzate") and 4.1 ("estensione del numero di dottorati di ricerca e dottorati innovativi per la pubblica amministrazione e il patrimonio culturale"), DM 351 of April 09, 2022 (scholarship no. 38-413-23-DOT20PA4JT-1070; CUP: J93C22001450005). E.-M.P. was funded by the Erasmus+ program for training at the Aristotle University of Thessaloniki, Greece (ER/SMP-OUT/2020-0122). L.S. is supported by a Humboldt Research Fellowship provided by the Alexander von Humboldt Foundation. M.B. collected metrical data on part of the *Pseudodama* populations used in the comparison under a Marie Curie Intra European Fellowship of the 7th FP (contract number 237010 - Deer Paleobiology) and a Synthesys-financed stay in Weimar (DE-TAF-5501). L.S. and S.B.L. thank CERCA Programme, Generalitat de Catalunya funds. B.M.-N. thanks the Spanish Ministry of Science and Innovation through the "María de Maeztu" excellence accreditation (CEX2019-000945-M) and the Generalitat de Catalunya, 2021SGR 01238 (AGAUR). E.-M.P. thanks David M. Alba and Josep M. Robles for their availability and kindness during the study of the collections of *Dama*-like deer hosted in the Institut Català de Paleontologia Miquel Crusafont; Javier Quesada for the possibility to study *Dama* collections from the Museu de Ciències Naturals de Barcelona. We thank Roman Croitor and an anonymous reviewer who helped to significantly improve the manuscript.

Appendix A. Supplementary data

Supplementary data to this article can be found online at https://doi.org/10.1016/j.qsa.2025.100294.

Data availability

Data will be made available on request.

References

Abbazzi, L., 2010. La fauna de cérvidos de Barranco León y Fuente Nueva 3. In: Toro, I.I., Martínez-Navarro, B., Agustí, J. (Eds.), Ocupaciones humanas en el Pleistoceno inferior y medio en la Cuenca de Guadix-Baza. Arqueología Monografías, Sevilla, pp. 273–290.
Abbazzi, L., Ficcarelli, G., Torre, D., 1995. Deer fauna from the Aulla quarry (Val di Magra, Northern Apennines). Biochronological remarks. Riv. Ital. Paleontol. Stratigr. 101 (3), 341–348.
Arzarello, M., Pavia, G., Peretto, C., Petronio, C., Sardella, R., 2012. Evidence of an early pleistocene hominin presence at Pirro Nord (Apricena, Foggia, southern Italy): P13 site. Quat. Int. 267, 56–61.
Athanassiou, A., 2022. The fossil record of continental fossil deer (Mammalia: Artiodactyla: Cervidae) in Greece. In: Vlachos, E. (Ed.), Fossil Vertebrates of Greece. Laurasiatherians, Artiodactyles, Perissodactyles, Carnivorans, and Island Endemics. 2. Springer International Publishing, Cham, pp. 205–247. In: .
Azzaroli, A., 1947. I cervi fossili della Toscana, con particolare riguardo alle specie villafranchiane. Palaeontogr. Ital. 43, 45–82.
Azzaroli, A., 1992. The cervid genus *Pseudodama* n.g. in the Villafranchian of Tuscany. Palaeontogr. Ital. 79, 1–41.
Azzaroli, A., 2001. On fossil deer from the Valdarno, Tuscany, Italy (comments on a paper by di Stefano & Petronio). N. Jb. Geol. Paläont. Mh. 3, 168–174.
Bedetti, C., Pavia, M., 2013. Early pleistocene birds from Pirro Nord (Puglia, southern Italy). Palaeont. Abt. A. 298, 31–53.
Bellucci, L., Sardella, R., Rook, L., 2015. Large mammal biochronology framework in Europe at Jaramillo: the Epivillafranchian as a formal biochron. Quat. Int. 389, 84–89.
Bertini, A., 2000. Pollen record from Colle Curti and Cesi: early and middle pleistocene mammal sites in the umbro-marchean apennine mountains (central Italy). J. Quat. Sci. 15, 825–840.
Bertini, A., 2010. Pliocene to Pleistocene palynoflora and vegetation in Italy: state of the art. Quat. Int. 225 (1), 5–24.
Bertini, A., Magi, M., Mazza, P.P., Fauquette, S., 2010. Impact of short-term climatic events on latest Pliocene land settings and communities in Central Italy (Upper Valdarno basin). Quat. Int. 225 (1), 92–105.
Blain, H.A., Fagoaga, A., Ruiz-Sánchez, F.J., Bisbal-Chinesta, J.F., Delfino, M., 2019. Latest Villafranchian climate and landscape reconstructions at Pirro Nord (southern Italy). Geology 47 (9), 829–832.
Böhme, M., 2020. New results on amphibians and reptiles from the Early Pleistocene site of Untermassfeld – Bioclimatic analysis of the herpetofauna. In: Kahlke, R.D. (Ed.), Das Pleistozän von Untermassfeld bei Meiningen (Thüringen), vol. 4. Monographien des RGZM, pp. 1141–1158.
Bona, F., Sala, B., 2016. Villafranchian-galerian mammal faunas transition in south-western Europe. The case of the late early pleistocene mammal fauna of the Frantoio locality, Arda River (Castell'Arquato, piacenza, northern Italy). Geobios 754, 1–19.
Bout, P., Azzaroli, A., 1952. Stratigraphie et faune du Creux de Peyrolles près Perrier (Puy-de-Dôme). Ann. Paleontol. 38, 37–56.
Breda, M., 2015. The early Middle Pleistocene fallow deer *Dama roberti*: new insight on species morphology from a complete postcranial skeleton from Valdemino (northwestern Italy). Geol. J. 50 (3), 257–270.
Breda, M., Lister, A.M., 2013. *Dama roberti*, a new species of deer from the early Middle Pleistocene of Europe, and the origins of modern fallow deer. Quat. Sci. Rev. 69, 155–167.
Breda, M., Peretto, C., Thun-Hohenstein, U., 2015. The deer from the early Middle Pleistocene site of Isernia la Pineta (Molise, Italy): revised identifications and new remains from the last 15 years of excavation. Geol. J. 50 (3), 290–305.
Breda, M., Kahlke, R.D., Lister, A.M., 2020. New results on cervids from the early Pleistocene site of Untermassfeld. In: Kahlke, R.D. (Ed.), Das Pleistozän von Untermassfeld bei Meiningen (Thüringen), vol. 4. Monographien des RGZM, pp. 1197–1249.
Catalano, 1983. (Tesi) Osservazioni su *Dama nestii* MAJOR e *Cervus philisi* SCHAUB: analisi biometrica e comparazione morfologica dei denti e dello scheletro postcraniale. Sapienza University of Rome, Unpublished Dissertation.
Cauche, D., 2022. The Vallonnet cave on the northern Mediterranean border: a record of one of the oldest human presences in Europe. Anthropologie 126 (1), 102974.
Cherin, M., Azzarà, B., Breda, M., Ansoleaga, A.B., Buzi, C., Pandolfi, L., Pazzaglia, F., 2019. Large mammal remains from the early pleistocene site of Podere san Lorenzo (Perugia, central Italy). Riv. Ital. Paleontol. Stratigr. 125 (2), 489–515.
Cherin, M., Breda, M., Esattore, B., Hart, V., Turek, J., Porciello, F., Angeli, G., Holpin, S., Iurino, D.A., 2022. A Pleistocene Fight Club revealed by the palaeobiological study of the *Dama*-like deer record from Pantalla (Italy). Sci. Rep. 12, 13898.
Cherin, M., Basilici, G., Duval, M., Shao, Q., Sier, M.J., Parés, J.M., Gliozzi, E., Mazzini, I., Magri, D., Di Rita, F., Iurino, D.A., Azzarà, B., Margaritelli, G., Pazzaglia, F., 2023. The dawn of the late Villafranchian: paleoenvironment and age

of the Pantalla paleontological site (Italy; early pleistocene). Quat. Sci. Rev. 316, 108279.
Coltorti, M., Albianelli, A., Bertini, A., Ficcarelli, G., Laurenzi, M.A., Napoleone, G., Torre, D., 1998. The Colle Curti mammal site in the Colfiorito area (Umbria-Marchean Apennine, Italy): geomorphology, stratigraphy, paleomagnetism and palynology. Quat. Int. 47, 107–116.
Croitor, R., 2001. Functional morphology of small-sized deer from the Early and Middle Pleistocene of Italy: implication for paleolandscape reconstruction. In: Cavarretta, G., Gioia, P., Mussi, M., Palombo, M.R. (Eds.), La Terra Degli Elefanti-the World of Elephants – Proceedings of the 1st International Congress, Rome, pp. 97–102.
Croitor, R., 2006. Early pleistocene small-sized deer of Europe. Hellenic J. Geosci. 41, 89–117.
Croitor, R., 2012. Lower pleistocene ruminants from Monte Riccio (Tarquinia, Italy). Muzeul Olteniei Craiova. Oltenia. Studii şi comunicări. Ştiinţele Naturii 28 (1), 221–226.
Croitor, R., 2014. Deer from Late Miocene to Pleistocene of Western Palearctic: matching fossil record and molecular phylogeny data. Zitteliana 32, 115–153.
Croitor, R., 2018. Plio-Pleistocene deer of western Palearctic: taxonomy, systematics, phylogeny. Inst. Zoolog. Acad. Sci. Moldova. Chişinău.
De Giuli, C., Masini, F., Torre, D., 1986. The Latest Villafranchian Faunas in Italy: the Pirro Nord Fauna (Apricena, Gargano). Paleontogr. Ital. 74, 51–62.
De Lumley, H., Kahlke, H.D., Moigne, A.M., Moullé, P.E., 1988. Les faunes de grands mammiferes de la Grotte du Vallonnet Roquebrune-Cap-Martin, Alpes-Maritimes. Anthropologie 92 (2), 465–496.
Di Stefano, G., Petronio, C., 1998. Origin of and relationships among the *Dama*-like cervids in Europe. Neues Jahrb. Geol. Palaeontol. Abh. 207 (1), 37–55.
Di Stefano, G., Petronio, C., 2002. Systematics and evolution of the Eurasian Plio-Pleistocene tribe Cervini (Artiodactyla, Mammalia). Geol. Rom. 36, 311–334.
Driesch, A. von den, 1976. A Guide to the Measurement of Animal Bones from Archaeological Sites. Peabody Museum Bulletin, Harvard.
Dubois, E., 1904. On an equivalent of the Cromer ForestBed in the Netherlands. Koninklijke Akademie van Wetenschappen. Proceedings Sect. Sci. 7 (3), 214–222.
Duval, M., Arnold, L.J., Bahain, J.J., Parés, J.M., Demuro, M., Falguères, C., Shao, Q., Voinchet, P., Arnaud, J., Berto, C., Berruti, G.L.F., Daffara, S., Sala, B., Arzarello, M., 2024. Re-examining the earliest evidence of human presence in western Europe: new dating results from Pirro Nord (Italy). Quat. Geochronol. 82, 101519.
Esattore, B., Saggiomo, L., Sensi, M., Francia, V., Cherin, M., 2022. Tell me what you eat and I'll tell you… where you live: an updated review of the worldwide distribution and foraging ecology of the fallow deer (*Dama dama*). Mamm. Biol. 102 (2), 321–338.
Ficcarelli, G., Mazza, P., 1990. New fossil findings from the Colfiorito basin (Umbria-Marchean Apennine). Boll. Soc. Paleontol. Ital. 29 (2), 245–247.
Ficcarelli, G., Silvestrini, M., 1991. Biochronologic remarks on the local fauna of Colle Curti (Colfiorito basin, Umbrian-Marchean Apennine, central Italy). Boll. Soc. Paleontol. Ital. 30 (2), 197–200.
Fidalgo, D., Rosas, A., Bartolini-Lucenti, S., Boisserie, J.R., Pandolfi, L., Martínez-Navarro, B., Palmqvist, P., Rook, L., Madurell-Malapeira, J., 2023. Increase on environmental seasonality through the European Early Pleistocene inferred from dental enamel hypoplasia. Sci. Rep. 13 (1), 16941.
Filella, J.B., Morán, F., Kemp, Y.J., Munir, H., Gort-Esteve, A., Cassinello, J., 2024. Diet comparison between sympatric European bison, red deer and fallow deer in a Mediterranean landscape. Biodivers. Conserv. 33 (5), 1775–1791.
Gabarda, M.V., Valle, R.M., Calatayud, P.G., Martí, P.G., Pueyo, E., Casabó, J., 2016. The Lower Palaeolithic site Alto de las Picarazas (Andilla-Chelva,Valencia). Quat. Int. 393, 83–94.
Gliozzi, E., Abbazzi, L., Argenti, P., Azzaroli, A., Caloi, L., Capasso Barbato, L., Di Stefano, G., Esu, D., Ficcarelli, G., Girotti, O., Kotsakis, T., Masini, F., Mazza, P., Mezzabotta, C., Palombo, M.R., Petronio, C., Rook, L., Sala, B., Sardella, R., Zanalda, E., Torre, D., 1997. Biochronology of selected mammals, molluscs and ostracods from the Middle Pliocene to the Late Pleistocene in Italy. The state of art. Riv. Ital. Paleontol. Stratigr. 103 (3), 369–388.
Hammer, Ø., Harper, D.A.T., Ryan, P.D., 2001. PAST: paleontological statistics software package for education and data analysis. Palaeontol. Electron. 4 (1), 9.
Heckeberg, N.S., 2020. The systematics of the Cervidae: a total evidence approach. PeerJ 8, e8114.
Head, M.J., Gibbard, P.L., 2015. Early–Middle Pleistocene transitions: linking terrestrial and marine realms. Quat. Int. 389, 7–46.
Heintz, E., 1970. Les cervidés villafranchiens de France et d'Espagne. Mém. Mus. natl. hist. nat., Sér. C Sci. terre 22.
Janis, C.M., 1990. Correlation of cranial and dental variables with body size in ungulates and macropodoids. In: Damuth, J., MacFadden, B.J. (Eds.), Body Size in Mammalian Paleobiology. Cambridge Univ. Press, Cambridge, UK, pp. 255–300.
Kahlke, H.-D., 1997. Die Cerviden-Reste aus dem Unterpleistozän von Untermassfeld. In: Kahlke, R.-D. (Ed.), Das Pleistozän von Untermassfeld bei Meiningen (Thüringen), vol. 1. Monographien des RGZM 40 (1), pp. 181–275.
Kahlke, H.-D., 2001. Neufunde von Cerviden-Resten aus dem Unterpleistozanen von Untermassfeld. In: Kahlke, R.-D. (Ed.), Das Pleistozän von Untermassfeld bei Meiningen (Thüringen), vol. 2. Monographien des RGZM 40 (2), pp. 461–482.
Kahlke, R.-D., 2009. Les communautés de grands mammifères du Pléistocène inférieur terminal et le concept d'un biochrone Épivillafranchien. Quaternaire 20 (4), 415–427.
Kahlke, R.D., García, N., Kostopoulos, D.S., Lacombat, F., Lister, A.M., Mazza, P.P., Spassov, N., Titov, V.V., 2011. Western Palaearctic palaeoenvironmental conditions during the Early and early Middle Pleistocene inferred from large mammal communities, and implications for hominin dispersal in Europe. Quat. Sci. Rev. 30 (11–12), 1368–1395.
Kahlke, R.D., 2022. The Pleistocene of Untermassfeld–a synopsis of site origin, palaeobiodiversity, taphonomic characteristics, palaeoanvironment, chronostratigraphy, and significance in western Palaearctic faunal history. In: Kahlke, R.D. (Ed.), The Pleistocene of Untermassfeld Near Meiningen (Thüringen, Germany), Monographien des RGZM 40 (5), pp. 1635–1734.
Kindler, L., Smith, G.M., García Moreno, A., Gaudzinski-Windeheuser, S., Roebroeks, W., 2020. The last interglacial (Eemian) lakeland of Neumark-Nord (Saxony-Anhalt, Germany). Sequencing Neanderthal occupations, assessing subsistence opportunities and prey selection based on estimations of ungulate carrying capacities, biomass production and energy. In: García-Moreno, A., Hutson, J.M., Smith, G.M., Turner, E., Villaluenga, A., Gaudzinski-Windheuser, S. (Eds.), Human Behavioural Adaptations to Interglacial Lakeshore Environments, 37. RGZM – Tagungen, Mainz und Heidelberg, pp. 67–104.
Konidaris, G.E., Kostopoulos, D.S., 2024. The late Pliocene–Middle Pleistocene Large Mammal Faunal Units of Greece. Quaternary 7 (2), 27.
Kostopoulos, D.S., 1997. The Plio-Pleistocene artiodactyls from Macedonia, Greece: 2. The fossiliferous locality of Volakas, VOL (Volakas basin, Drama, NE Greece). Paleontol. Evol. 30–31, 83–92.
Kostopoulos, D.S., Athanassiou, A., 2005. In the shadow of bovids: suids, cervids and giraffids from the Plio-Pleistocene of Greece. In: Crégut- Bonnoure, E. (Ed.), Les ongulés holarctiques du Pliocène et du Pléistocène. Quaternaire hors-série 2, 179–190.
Koufos, G.D., Kostopoulos, D.S., 2016. The Plio-Pleistocene large mammal record of Greece: implications for early human dispersals into Europe. In: Harvati, K., Roksandic, M. (Eds.), Paleoanthropology of the Balkans and Anatolia: Human Evolution and its Context. Springer, Dordrecht, pp. 269–280.
Laurat, T., Brühl, E., 2021. Neumark-Nord 2–a multiphase Middle Palaeolithic open-air site in the Geisel Valley (Central Germany). Anthropologie 125 (4), 102936.
Leroy, S.A., Arpe, K., Mikolajewicz, U., 2011. Vegetation context and climatic limits of the Early Pleistocene hominin dispersal in Europe. Quat. Sci. Rev. 30 (11–12), 1448–1463.
Lisiecki, L.E., Raymo, M.E., 2007. Plio–Pleistocene climate evolution: trends and transitions in glacial cycle dynamics. Quat. Sci. Rev. 26 (1–2), 56–69.
Lister, A.M., 1996. The morphological distinction between bones and teeth of fallow deer (*Dama dama*) and red deer (*Cervus elaphus*). Int. J. Osteoarchaeol. 6, 119–143.
Lister, A.M., Parfitt, S.A., Owen, F.J., Collinge, S.E., Breda, M., 2010. Metric analysis of ungulate mammals in the early Middle Pleistocene of Britain, in relation to taxonomy and biostratigraphy: II: Cervidae, Equidae and Suidae. Quat. Int. 228 (1–2), 157–179.
Lopez-Garcia, J.M., Luzi, E., Berto, C., Peretto, C., Arzarello, M., 2015. Chronological context of the first hominin occurrence in southern Europe: the *Allophaiomys ruffoi* (Arvicolinae, Rodentia, Mammalia) from Pirro 13 (Pirro Nord, Apulia, southwestern Italy). Quat. Sci. Rev. 107, 260–266.
Made, J. Van der, 1999. Ungulates from Atapuerca TD6. J. Hum. Evol. 37, 389–413.
Made, J. Van der, 2001. Les Ongulés d'Atapuerca. Stratigraphie et biogéographie. L'Anthropologie 105 (1), 95–113.
Made, J. Van der, 2013. First description of the large mammals from the locality of Penal, and updated faunal lists for the Atapuerca ungulates–*Equus altidens, Bison* and human dispersal into Western Europe. Quat. Int. 295, 36–47.
Made, J. Van der, 2015. The latest Early Pleistocene giant deer *Megaloceros novocarthaginiensis* n. sp. and the fallow deer *Dama* cf. *vallonnetensis* from Cueva Victoria (Murcia, Spain). MASTIA 11–12–13, 269–323.
Made, J. Van der, Rodríguez-Alba, J.J., Martos, J.A., Gamarra, J., Rubio-Jara, S., Panera, J., Yravedra, J., 2023. The fallow deer *Dama celiae* sp. nov. with two-pointed antlers from the Middle Pleistocene of Madrid, a contemporary of humans with Acheulean technology. Archaeol. Anthropol. Sci. 15 (4), 41.
Made, J. Van der, Rosell, J., Blasco, R., 2017. Faunas from Atapuerca at the Early–Middle Pleistocene limit: the ungulates from level TD8 in the context of climatic change. Quat. Int. 433, 296–346.
Made, J. Van der, Stefaniak, K., Marciszak, A., 2014. The Polish fossil record of the wolf *Canis* and the deer *Alces, Capreolus, Megaloceros, Dama* and *Cervus* in an evolutionary perspective. Quat. Int. 326, 406–430.
Madurell-Malapeira, J., 2022. El Vilafranquià a Catalunya: glaciacions i grans carnívors. Quaderns de les Assemblees d'estudis de Besalú 3, 9–44.
Madurell-Malapeira, J., 2023. 25 anys de treballs a la Secció de Vallparadís (Terrassa). Cicle de conferències de la Tribuna d'Arqueologia, Generalitat de Catalunya. Departament de Cultura, pp. 1–4.
Madurell-Malapeira, J., Minwer-Barakat, R., Alba, D.M., Garcés, M., Gómez, M., Aurell-Garrido, J., Ros-Montoya, S., Moyà-Solà, S., Berástegui, X., 2010. The Vallparadís section (Terrassa, Iberian peninsula) and the latest Villafranchian faunas of Europe. Quat. Sci. Rev. 29 (27–28), 3972–3982.
Madurell-Malapeira, J., Alba, D.M., Minwer-Barakat, R., Aurell-Garrido, J., Moyà-Solà, S., 2012. Early human dispersals into the Iberian Peninsula: A comment on Martínez et al. (2010) and Garcia et al. (2011). J. Hum. Evol. 62 (1), 169–173.
Madurell-Malapeira, J., Ros-Montoya, S., Espigares-Ortiz, M.P., Alba, D.M., Aurell-Garrido, J., 2014. Villafranchian large mammals from the Iberian Peninsula: paleobiogeography, paleoecology and dispersal events. J. Iber. Geol. 40, 167–178.
Madurell-Malapeira, J., Alba, D.M., Espigares, M.P., Vinuesa, V., Palmqvist, P., Martínez-Navarro, B., Moya-Sola, S., 2017. Were large carnivorans and great climatic shifts limiting factors for hominin dispersals? Evidence of the activity of *Pachycrocuta brevirostris* during the Mid-Pleistocene Revolution in the Vallparadís Section (Vallès-Penedès Basin, Iberian Peninsula). Quat. Int. 431, 42–52.
Madurell-Malapeira, J., Sorbelli, L., Bartolini Lucenti, S., Ruffí, I., Prat-Vericat, M., Ros-Montoya, S., Espigares, M.P., Martínez-Navarro, B., 2019. The Iberian latest Early

Pleistocene: glacial pulses, large carnivorans and hominins. In: Martínez-Navarro, B., Palmqvist, P., Espigares, M.P., Ros-Montoya, S. (Eds.), Libro de Resúmenes XXXV Jornadas de la Sociedad Española de Paleontología, Granada, pp. 155–159.
Madurell-Malapeira, J., Prat-Vericat, M., Bartolini-Lucenti, S., Faggi, A., Fidalgo, D., Marciszak, A., Rook, L., 2024. A review on the latest early pleistocene carnivoran guild from the Vallparadís section (NE Iberia). Quaternary 7 (3), 40.
Magri, D., Palombo, M.R., 2013. Early to Middle Pleistocene dynamics of plant and mammal communities in south west Europe. Quat. Int. 288, 63–72.
Magri, D., Di Rita, F., Aranbarri, J., Fletcher, W., González-Sampériz, P., 2017. Quaternary disappearance of tree taxa from Southern Europe: timing and trends. Quat. Sci. Rev. 163, 23–55.
Mancini, M., Bellucci, L., Petronio, C., 2008. Il Pleistocene Inferiore e Medio di Nettuno (Lazio): Stratigrafia e Mammalofauna. Geol. Rom. 41, 71–85.
Martínez-Navarro, B., Montoya, S.R., Ortiz, M.P.E., Madurell-Malapeira, J., Palmqvist, P., 2018. Los mamíferos del Plioceno y Pleistoceno de la Península Ibérica. Boletín del Instituto Andaluz del Patrimonio Histórico 26 (94), 206–249.
Mazza, P.P.A., Ventra, D., 2011. Pleistocene debris-flow deposition of the hippopotamus-bearing Collecurti bonebed (Macerata, Central Italy): taphonomic and paleoenvironmental analysis. Palaeogeogr. Palaeoclimatol. Palaeoecol. 310 (3–4), 296–314.
Mecozzi, B., Sardella, R., Breda, M., 2023. Late Early to late Middle Pleistocene medium-sized deer from the Italian Peninsula: implications for taxonomy and biochronology. Paleobiodivers. Paleoenviron. 1–25.
Menéndez, E., 1987. Cervidos del yacimiento del Pleistoceno inferior de Venta Micena-2, Orce (Granada, España). Paleontologia i Evolució. Memoria Especial 1, 129–181.
Michel, V., Shen, C.C., Woodhead, J., Hu, H.M., Wu, C.C., Moullé, P.É., Khatib, S., Cauche, D., Moncel, M.H., Valensi, P., Chou, Y.M., 2017. New dating evidence of the early presence of hominins in Southern Europe. Sci. Rep. 7 (1), 10074.
Mijarra, J.M.P., Burjachs, F., Manzaneque, F.G., Morla, C., 2007. A palaeoecological interpretation of the lower–middle Pleistocene Cal Guardiola site (Terrassa, Barcelona, NE Spain) from the comparative study of wood and pollen samples. Rev. Palaeobot. Palynol. 146 (1–4), 247–264.
Minwer-Barakat, R., Madurell-Malapeira, J., Alba, D.M., Aurell-Garrido, J., De Esteban-Trivigno, S., Moyà-Solà, S., 2011. Pleistocene rodents from the Torrent de Vallparadís section (Terrassa, northeastern Spain) and biochronological implications. J. Vertebr. Paleontol. 31 (4), 849–865.
Moullé, P.E., 1990. Les cervidés de la grotte du Vallonnet (Roquebrune- Cap-Martin, Alpes-Maritimes). Quaternaire 1, 193–196.
Moullé, P.-E., 1992. Grands mammifères du Pléistocène inférieur de la grotte du Vallonnet (Roquebrune-Cap-Martin, Alpes Maritimes). Etude paleontologique des carnivores, Equidés, Suidés et Bovidés. Muséum National d'Histoire Naturelle, Paris.. Ph.D. Dissertation.
Moullé, P.E., Lacombat, F., Echassoux, A., 2006. Apport des grands mammifères de la grotte du Vallonnet (Roquebrune-Cap-Martin, Alpes-Maritimes, France) à la connaissance du cadre biochronologique de la seconde moitié du Pléistocène inférieur d'Europe. Anthropologie 110, 837–849.
Pacheco, F.G., Santiago, A., Gutiérrez, J.M., López-García, J.M., Blain, H.-A., Cuenca-Bescós, G., Made, J. Van der, Cáceres, I., García, N., 2011. The Early Pleistocene paleontological site in the Sierra del Chaparral (Villaluenga del Rosario, Cádiz, Southwestern Spain). Quat. Int. 243 (1), 92–104.
Palombo, M.R., Valli, A.M.F., 2003. Remarks on the biochronology of mammalian faunal complexes from the Pliocene to the Middle Pleistocene in France. Geol. Rom. 37 (2003–2004), 145–163.
Pavia, G., Zunino, M., Coltorti, M., Angelone, C., Arzarello, M., Bagnus, C., Bellucci, L., Colombero, S., Marcolini, F., Peretto, C., Petronio, C., Petrucci, M., Pieruccini, P., Sardella, R., Tema, E., Villier, B., Pavia, G., 2012. Stratigraphical and palaeontological data from the Early Pleistocene Pirro 10 site of Pirro Nord (Puglia, south eastern Italy). Quat. Int. 267, 40–55.
Petronio, C., 1979. *Dama nestii eurygonos* Azz. Di Capena. Geol. Rom. 18, 105–125.
Petronio, C., Bellucci, L., Martiinetto, E., Pandolfi, L., Salari, L., 2011. Biochronology and palaeoenvironmental changes from the middle Pliocene to the late pleistocene in Central Italy. Geodiversitas 33 (3), 485–517.
Petronio, C., Bellucci, L., Di Stefano, G., 2013. *Axis eurygonos* from Pirro Nord (Apricena, southern Italy). Palaeontogr. Abt. A. 298, 169–181.
Pfeiffer, T., 2005. The position of *Dama* (Cervidae, Mammalia) in the system of fossil and living deer from Europe- phylogenetical analysis based on the postcranial skeleton. In: Crégut- Bonnoure, E.Les ongulés holarctiques du Pliocène et du Pléistocène. Quaternaire, Hors-série 2, 39-57.
Pfeiffer-Deml, T., 2016. Deer from the Pliocene site of Bad Deutsch-Altenburg 26 (Lower Austria, Leithagebirge): conclusions based on skeletal morphology. Ann. Nat. Mus. Wien 118, 133–173.
Ramada, N., 2024. Palaecological Inferences through Stable Isotopes Analyses on the Early Pleistocene Large Mammal Assemblages from Pirro Nord (Apulia, Southern Italy) and Quibas (Murcia, SE Iberia). Universitat Autònoma de Barcelona. Unpublished master thesis.
Renault-Miskovsky, J., Girard, M., 1978. Analyse pollinique du remplissage pleistocène inférieur et moyen de la grotte du Vallonnet (Roquebrune—Cap-Martin, Alpe-Maritimes). Geol. Mediterr. 5 (4), 385–402.
Renault-Miskovsky, J., Lebreton, V., 2006. Place de la palynologie archéologique, au regard des longues séquences polliniques de référence. C. R. Palevol 5 (1–2), 73–83.
Rosas, A., Galli, E., Fidalgo, D., García Tabernero, A., Huguet, E., García-Martínez, D., Piñero, P., Agustí, J., Rico-Barrio, A., Vallverdú, J., 2022. The Quibas site (Murcia, Spain): new herbivores form the Early-Middle Pleistocene Transition. Riv. Ital. Paleontol. Stratigr. 128 (3), 745–772.
Saarinen, J., Oksanen, O., Žliobaitė, I., Fortelius, M., DeMiguel, D., Azanza, B., Bocherens, H., Luzón, C., Solano-García, J., Yravedra, J., Courtenay, L.A., Blain, H.-A., Sánchez-Bandera, C., Serrano-Ramos, A., Rodriguez-Alba, J.J., Viranta, S., Barsky, D., Tallavaara, M., Oms, O., Agustí, J., Ochando, J., Carrión, J.S., Jiménez-Arenas, J.M., 2021. Pliocene to Middle Pleistocene climate history in the Guadix-Baza Basin, and the environmental conditions of early *Homo* dispersal in Europe. Quat. Sci. Rev. 268, 107132.
Schreve, D.C., 2001. Differentiation of the British late Middle Pleistocene interglacials: the evidence from mammalian biostratigraphy. Quat. Sci. Rev. 20 (16–17), 1693–1705.
Sorbelli, L., Alba, D.M., Cherin, M., Moullé, P.É., Brugal, J.P., Madurell-Malapeira, J., 2021. A review on *Bison schoetensacki* and its closest relatives through the Early-Middle Pleistocene Transition: Insights from the Vallparadís Section (NE Iberian Peninsula) and other European localities. Quat. Sci. Rev. 261, 106933.
Sorbelli, L., Cherin, M., Kostopoulos, D.S., Sardella, R., Mecozzi, B., Plotnikov, V., Prat-Vericat, M., Azzarà, B., Bartolini-Lucenti, S., Madurell-Malapeira, J., 2023. Earliest bison dispersal in Western Palearctic: insights from the *Eobison* record from Pietrafitta (Early Pleistocene, central Italy). Quat. Sci. Rev. 301, 107923.
Steensma, K.J., 1988. PlioPleistozäne Großsäugetiere (Mammalia) aus dem Becken von Kastoria/Grevena, südlich von Neapolis. NW Griechenland. Technische Universität Clausthal. PhD Dissertation.
Stefanelli, D., Mecozzi, B., 2020. Body-mass estimation from Middle Pleistocene fallow deer of Europe. Fossilia 2020, 47–51.
Stefaniak, K., 2015. Neogene and Quaternary Cervidae from Poland. Institute of Systematics and Evolution of Animals, Polish Academy of Sciences, Kraków, p. 260.
Strani, F., DeMiguel, D., Bellucci, L., Sardella, R., 2018. Dietary response of Early Pleistocene ungulate communities to the climate oscillations of the Gelasian/Calabrian transition in Central Italy. Palaeogeogr. Palaeoclimatol. Palaeoecol. 499, 102–111.
Strani, F., DeMiguel, D., Alba, D.M., Moyà-Solà, S., Bellucci, L., Sardella, R., Madurell-Malapeira, J., 2019. The effects of the "0.9 Ma event" on the Mediterranean ecosystems during the Early-Middle Pleistocene transition as revealed by dental wear patterns of fossil ungulates. Quat. Sci. Rev. 210, 80–89.
Strani, F., Di Folco, F., Iurino, D.A., Cherin, M., Pushkina, D., Rook, L., Sardella, R., Azanza, B., DeMiguel, D., 2024. Neuroanatomy and palaeoecology of the Early Pleistocene *Dama*-like deer from Pirro Nord (Apulia, Italian Peninsula). Quat. Sci. Rev. 334, 108719.
Valli, A.M.F., Caron, J.-B., Debard, E., Guérin, C., Pastre, J.-F., Argant, J., 2006. Le gisement paléontologique villafranchien terminal de Peyrolles (Issoire, Puy-de-Dôme, France) : résultats de nouvelles prospections. Geodiversitas 28 (2), 297–317.
Valli, A.M., 2025. New data on Cervidae (Mammalia, Artiodactyla) from the Villafranchian locality of Senèze (Haute-Loire, France). In: Delson, E., Sargis, E.J. (Eds.), Senèze: Life in Central France Around Two Million Years Ago. Springer Cham, pp. 409–431.
Vizcaíno-Varo, V., 2023. Paleoecology and Dietary Habits of Cave Bear Lineage through Stable Isotopes Analyses ($\delta^{13}C$ and $\delta^{18}O$) and Dental Microwear on *Ursus deningeri* from Vallparadís Section (Terrassa, Vallès-Penedès Basin, NE Iberian Peninsula). Universitat Rovira i Virgili. Unpublished master thesis.
Vos, J. de, Mol, D., Reumer, J.W.F., 1995. Early Pleistocene Cervidae (Mammalia, Artiodactyla) from the Oosterschelde (The Netherlands), with a revision of the cervid genus *Eucladoceros* Falconer. 1868. DElNSEA 2, 95–121.
Vos, J. de, Made, J. Van der, Athanassiou, A., Lyras, G., Sondaar, P.Y., Dermitzakis, M.D., 2002. Preliminary note on the late Pliocene fauna from Vatera (Lesvos, Greece). Ann. Geol. Pays Hell. 39, 37–70.
Walker, M.J., Haber Uriarte, M., López Jiménez, A., López Martínez, M., Martín Lerma, I., Made, J. Van der, Duval, M., Grün, R., 2020. Cueva Negra del Estrecho del Río Quípar: A dated late early pleistocene palaeolithic site in Southeastern Spain. J. Paleolit. Archaeol. 3 (4), 816–855.